Combining wind tunnel modeling and numerical simulation to study turbulence and dispersion in planetary boundary layer flows

Evgeni Fedorovich
School of Meteorology, University of Oklahoma, Norman, Oklahoma

Outline

- **Overview of neutral and convective atmospheric boundary layer flows reproduced in wind tunnels: a story of successes and challenges**
- **Using wind tunnel data for evaluation of simple models of dispersion from a line source in a neutral atmospheric surface layer**
- **Coupling wind tunnel experiment with LES to study turbulence and dispersion in an atmospheric convective boundary layer (CBL)**
- **Current state in the area and future outlook**

Triad of approaches in atmospheric boundary layer studies

I. Field observations/measurements

- *In situ*/contact measurements
- Remote sensing techniques

II. Physical/laboratory models

- Laboratory tank (thermal and saline) models
- Water channel models
- Wind tunnel (stratified and neutral) models

III. Theoretical/numerical techniques

- Theoretical/analytical models
- Numerical models/parameterizations
- Numerical simulations (direct and large-eddy)

I. Field observations/measurements

In situ/contact measurements and remote sensing techniques

Single global asset: it is real!

Hard or impossible to

- separate different contributing forcings/mechanisms,
- match temporal/spatial requirements for retrieval of statistics,
- control external forcings and boundary conditions,
- obtain accurate and complete data at low cost.

II. Physical/laboratory models

Laboratory tanks, water channels, wind tunnels

Pros:

- High level of complexity of modeled flows
- Controlled external/ boundary parameters
- Repeatability of flow regimes
- Possibility to generate well-documented data sets for evaluation of numerical models/simulations

Hard or impossible to

- reproduce several contributing forcings in combination,
- sufficiently match scaling/ similarity requirements in order to relate the modeled flow to its atmospheric prototype,
- find a reasonable balance between the value of results and cost of facility.

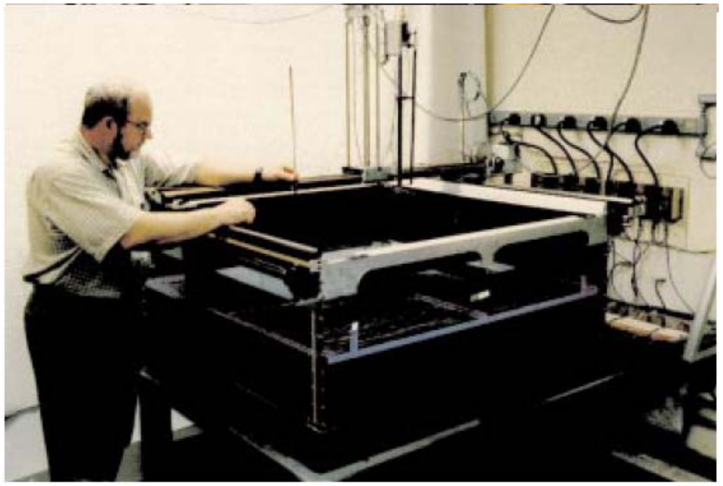

III. Theoretical/numerical techniques

Analytical models, numerical models/parameterizations, numerical simulations

$$\frac{\partial u_i}{\partial t}+\frac{\partial u_i u_j}{\partial x_j}=-\frac{1}{\rho}\frac{\partial p'}{\partial x_i}+b\delta_{i3}+\nu\frac{\partial^2 u_i}{\partial x_j \partial x_j}, \qquad \frac{\partial u_i}{\partial x_i}=0$$

Pros:

- Availability at a relatively low cost
- Capability to generate instantaneous flow fields
- Accounting for processes within relatively broad ranges of temporal and spatial scales

Hard or impossible to

- reproduce flow regimes with realistic environmental settings,
- evaluate precisely effects of subgrid/subfilter/ensemble turbulence closures,
- separate numerical artifacts from actual physical features of the modeled/simulated flows.

Wind tunnel modeling of neutral atmospheric BL flows

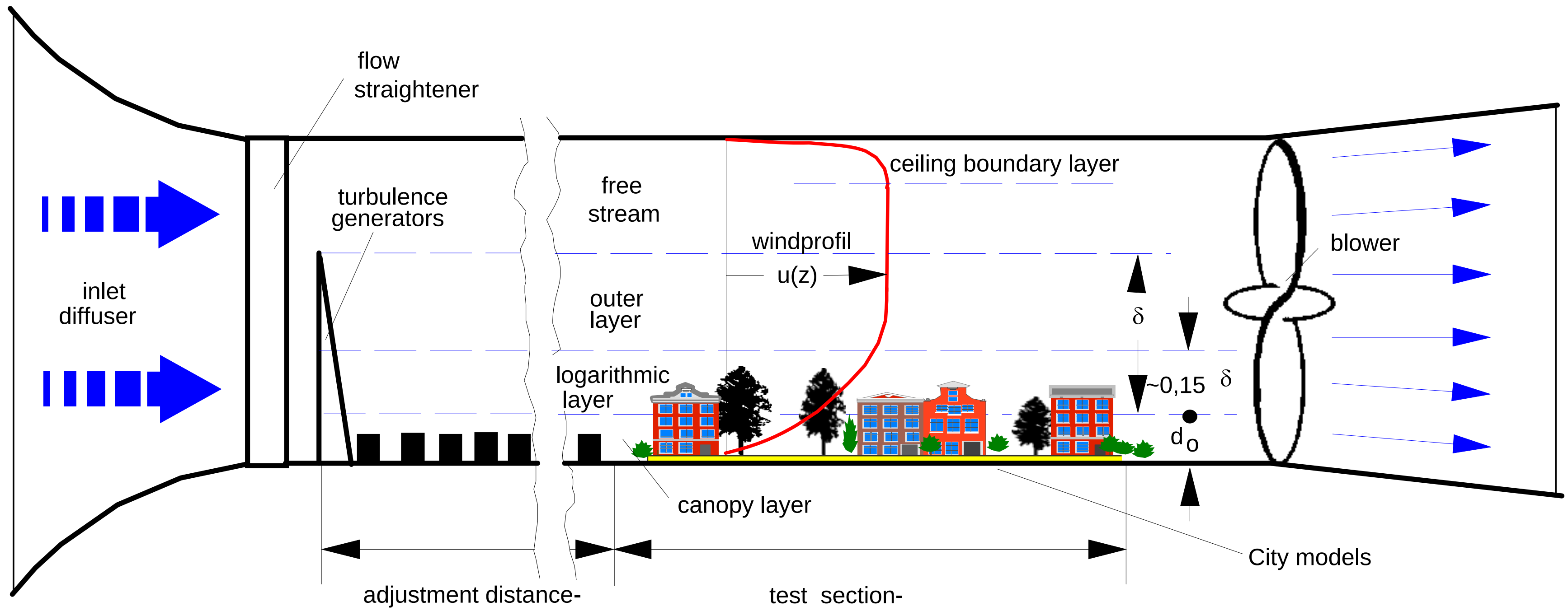

Design features of neutral boundary layer wind tunnels

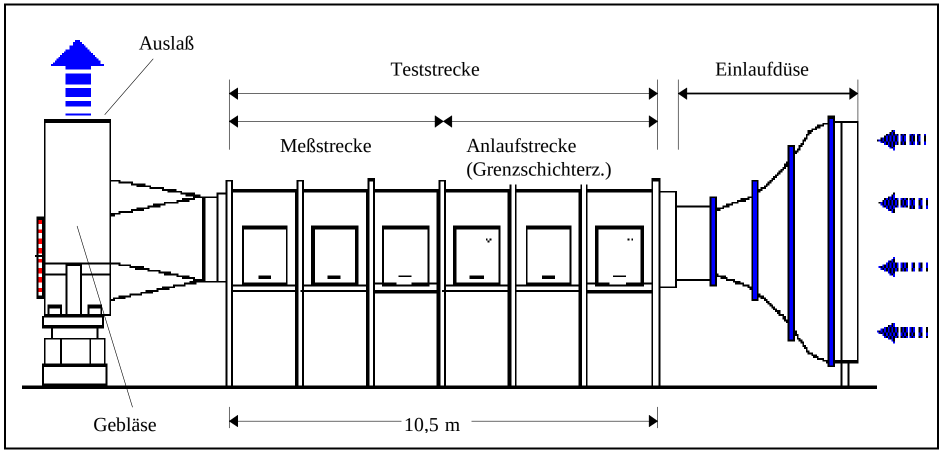

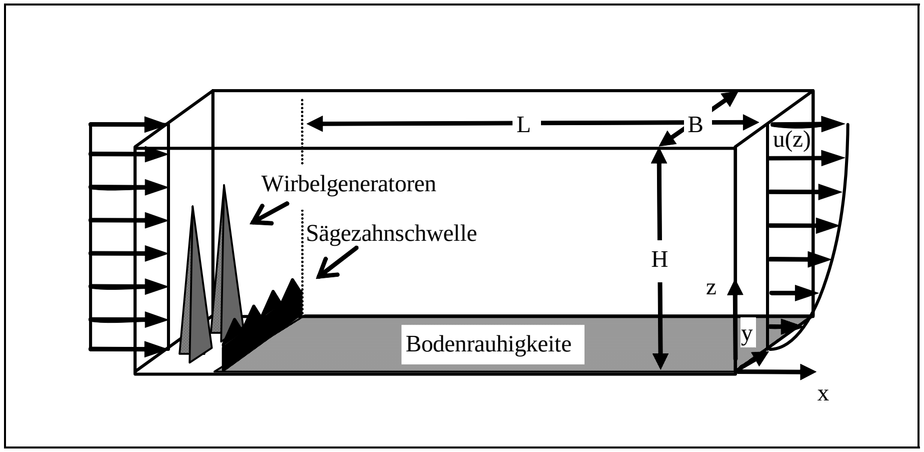

Interior of a modern neutral BL wind tunnel (WOTAN)

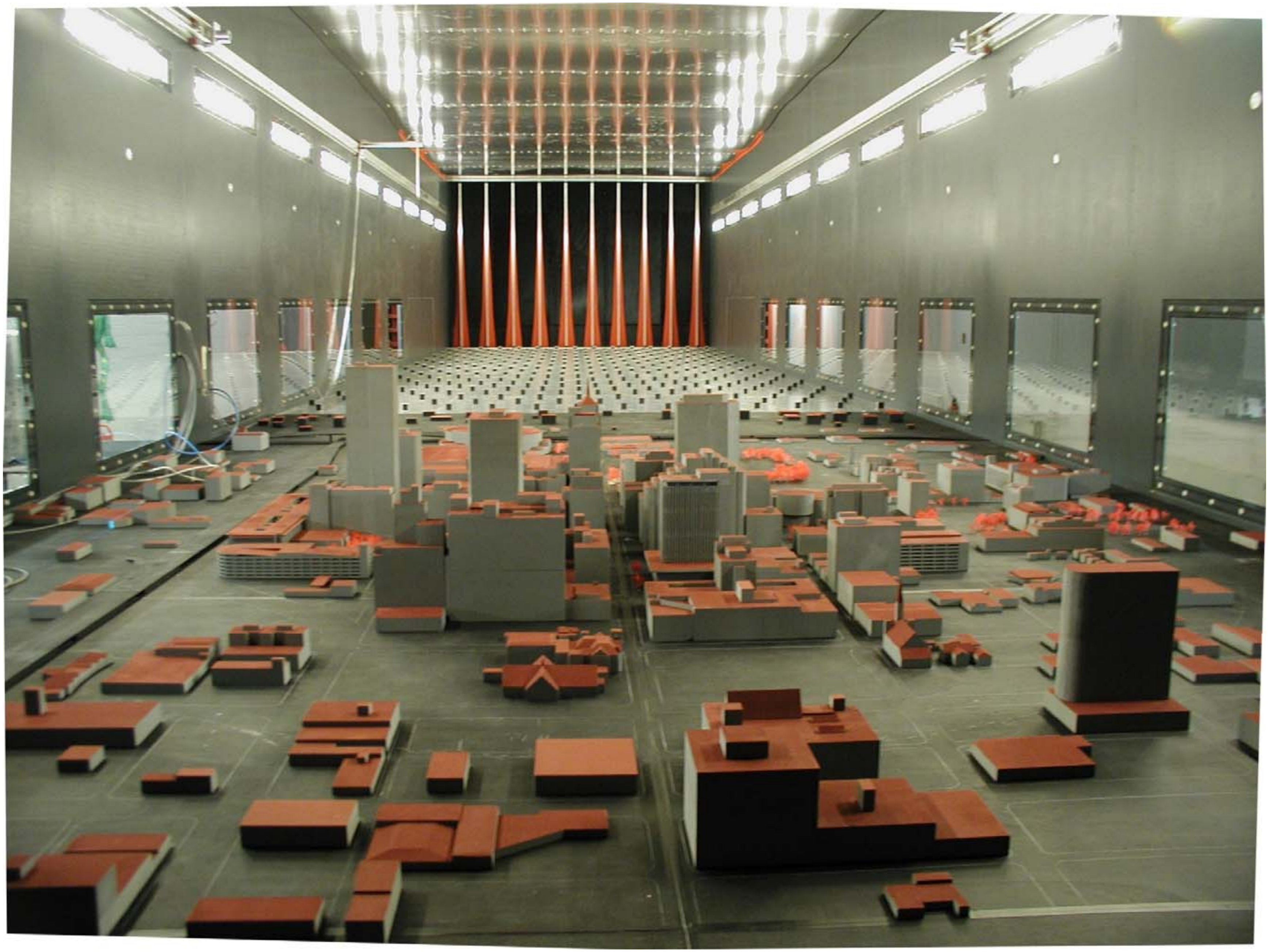

Similarity criteria for wind tunnel modeling of neutral BL flows

Length scales: $L_1 = z_0, \quad L_2 = d_0, \quad L_3 = \delta, \ldots$

Criteria: $(L_i / L_k)_{\text{model}} = (L_i / L_k)_{\text{nature}}$

Wind profile: $S_f = \dfrac{u(z)}{u_{\text{ref}}} = \left(\dfrac{z - d_0}{z_{\text{ref}} - d_0} \right)^{\alpha}, \; S_l = \dfrac{\kappa u(z)}{u_*} = \ln \dfrac{z - d_0}{z_0}$

Criteria: $S_{f\,\text{model}} = S_{f\,\text{nature}}, \; S_{l\,\text{model}} = S_{l\,\text{nature}}$

Turbulence intensity $I_i = \sigma_i / u_i$ **and spectra** $S_{ni} = k S_{ii}(k) / \sigma_i^2$

Criteria: $I_{i\,\text{model}} = I_{i\,\text{nature}}, \; S_{ni\,\text{model}} = S_{ni\,\text{nature}}$

Surface roughness in the model: $\text{Re}_0 = \dfrac{u_* z_0}{\nu} >> 1,$

where $u_* = (\tau_s / \rho)^{1/2} = \left(-\overline{u'w'}\Big|_s \right)^{1/2}$

Scaled mean wind profiles in WOTAN

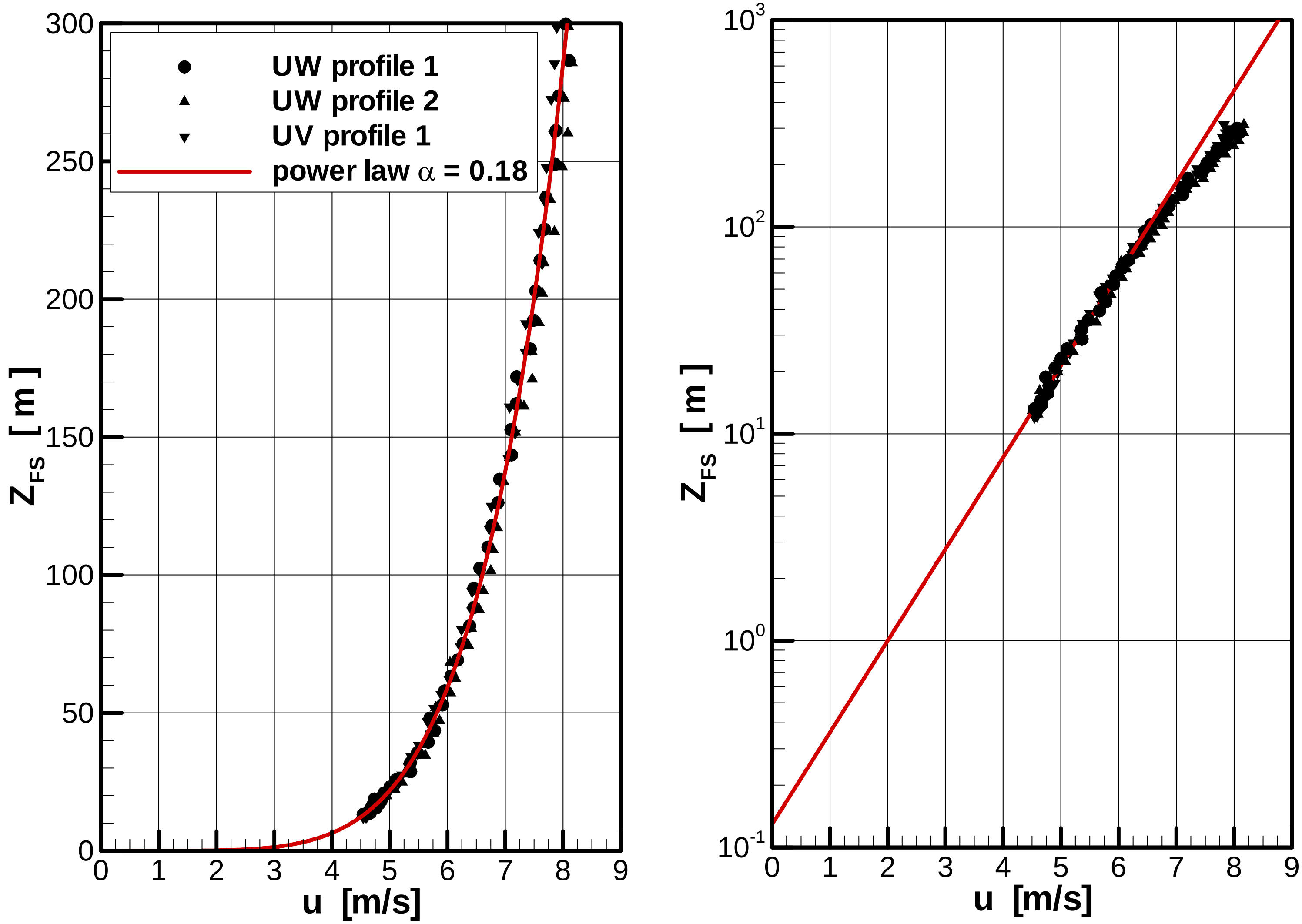

Intensities of turbulent velocity fluctuations in WOTAN

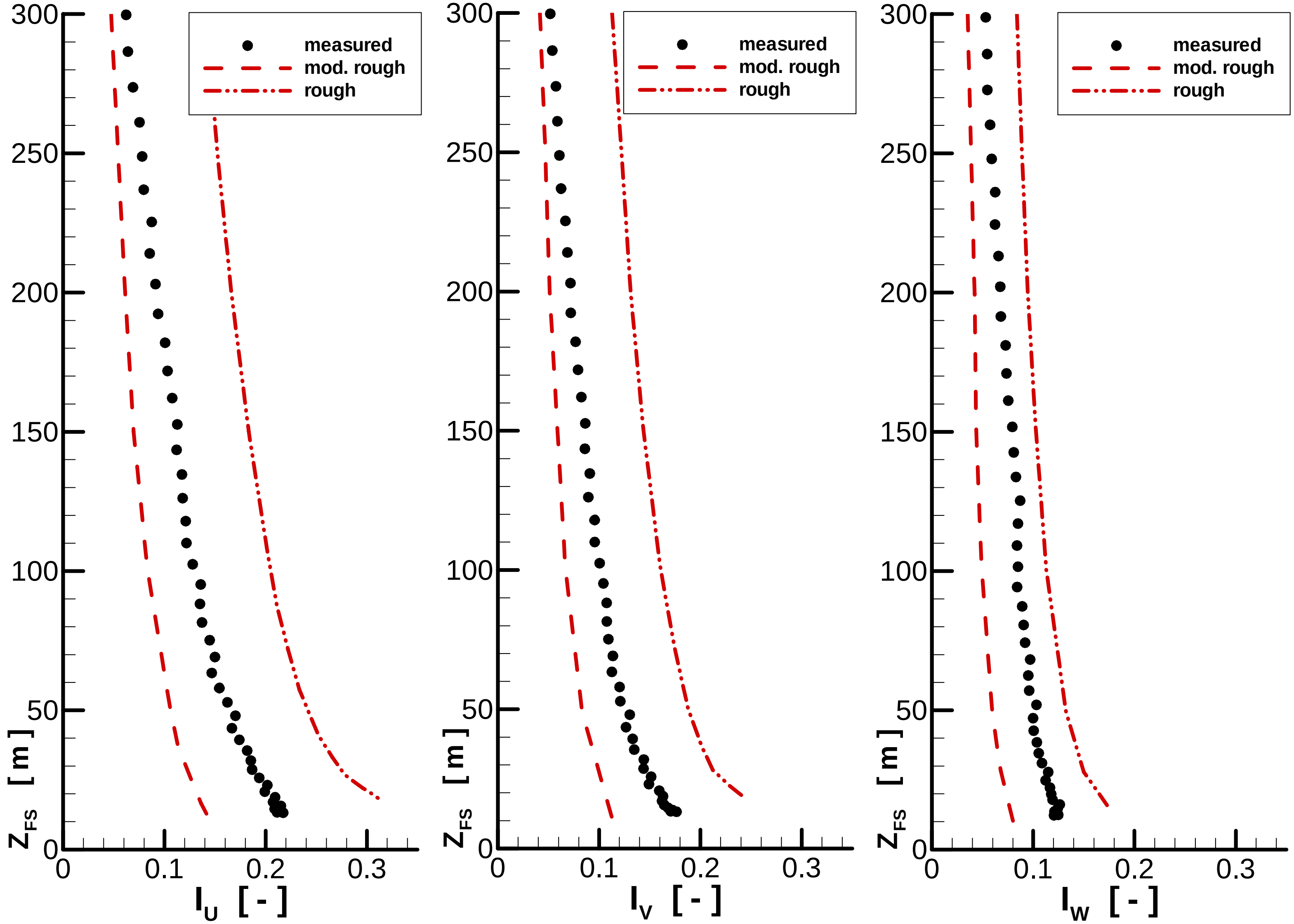

Longitudinal velocity component spectrum in WOTAN

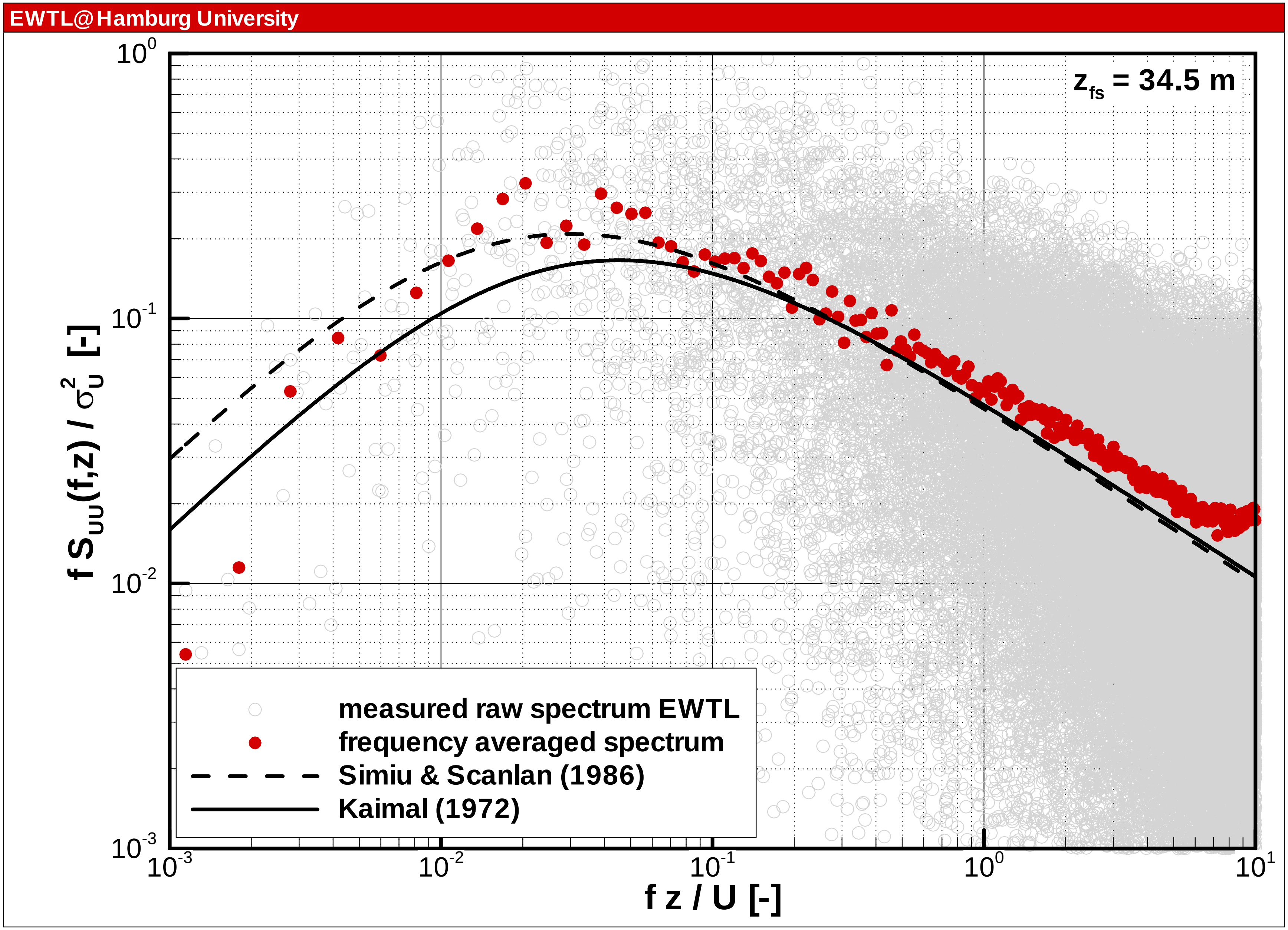

Vertical turbulent kinematic momentum flux in WOTAN

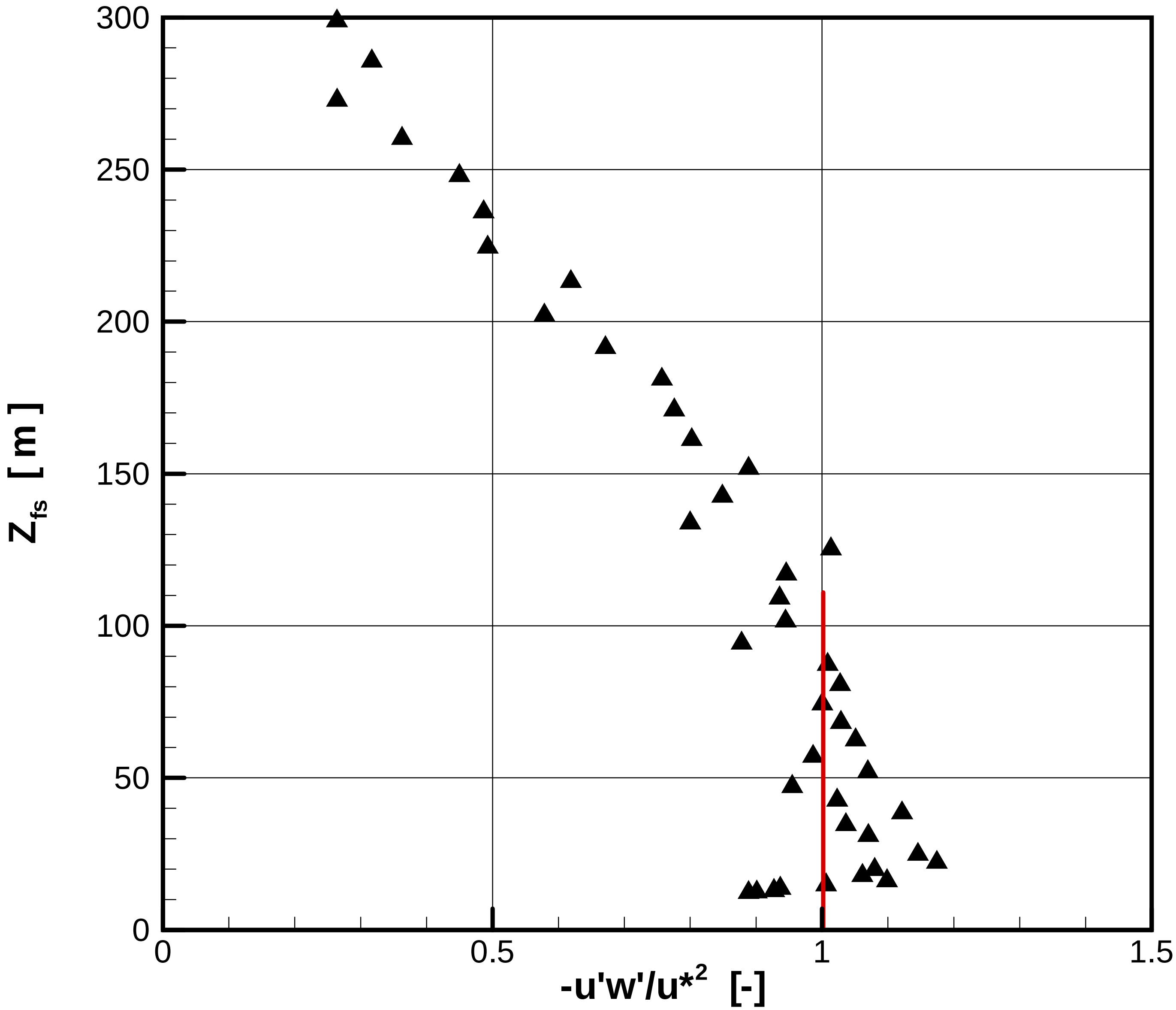

Flow parameters in the neutral boundary layer tunnel of UniKA

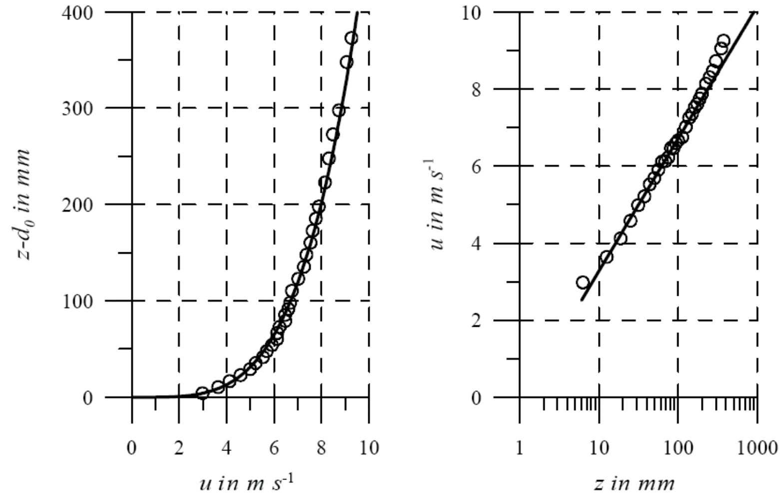

Fig. 1. Power-law (left diagram) and log-law (right diagram) approximations of the mean velocity profile measured in the wind-tunnel boundary layer (symbols).

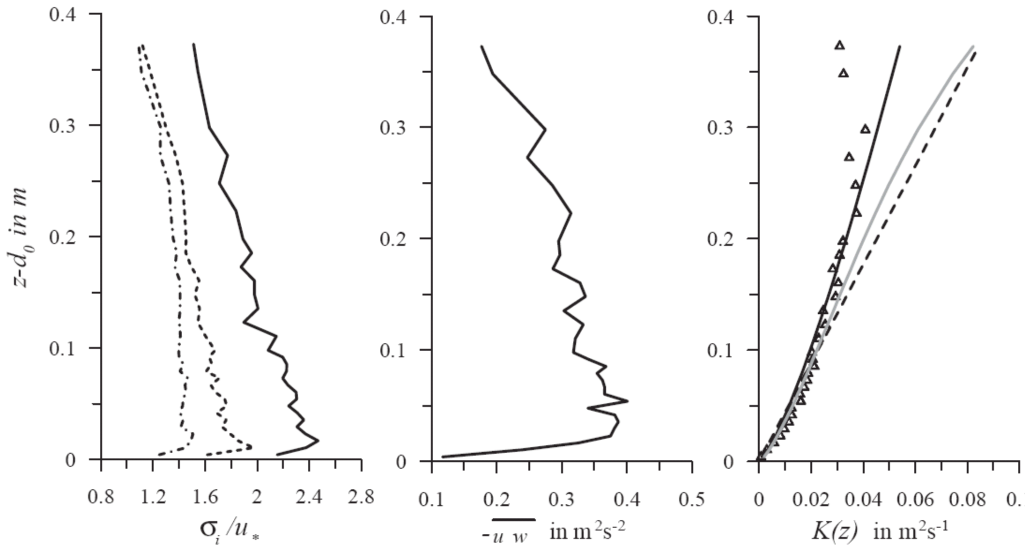

Fig. 2. Left plot: normalized velocity component rms fluctuations in the wind-tunnel flow; solid line shows σ_u, —— σ_v and - · - · - · - σ_w; central plot: turbulent momentum flux $-\overline{uw}$; right plot: turbulent diffusivity for momentum $K_m(z)$ in the wind-tunnel flow (symbols) compared to the similarity theory (black dashed line) and conjugate-power law (black solid line) $K_m(z)$ predictions. A turbulent diffusivity profile for a scalar, $K_c(z)$, calculated based on the conjugate-power-law expression for $K_m(z)$ and $Sc_t = 0.9 - 0.4(z/\delta)^2$ is shown by the gray line.

Dispersion of passive scalar from a ground line source

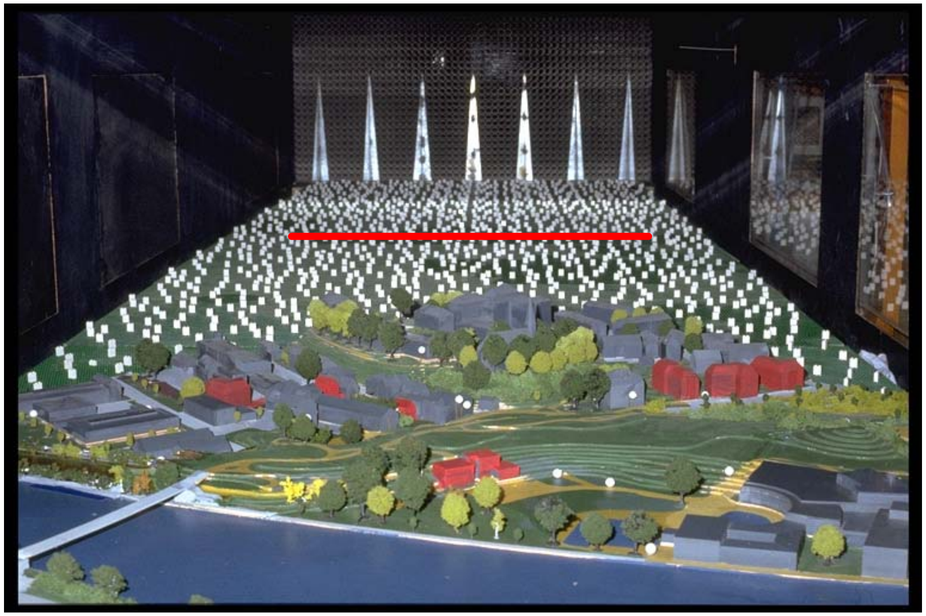

Schematic of the source (red line) deployed in the UniKA neutral WT

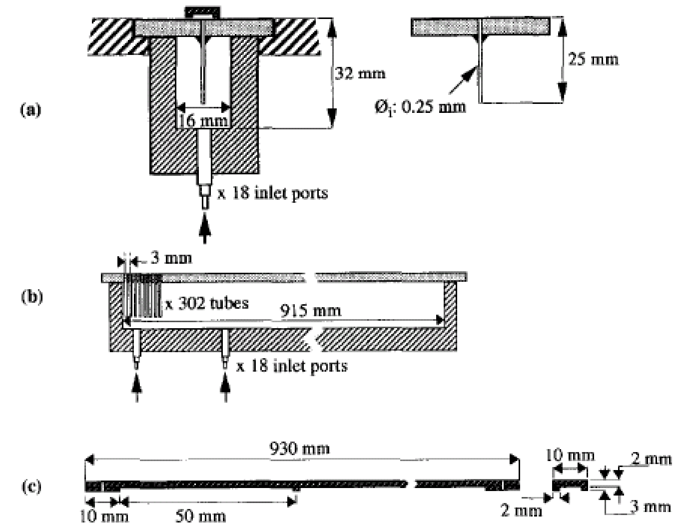

Fig. 6. Actual line source design. (a) Transverse cross section; (b) Longitudinal cross section; and (c) Capping brass bar.

Design of the line source after Meroney et al. (1996)

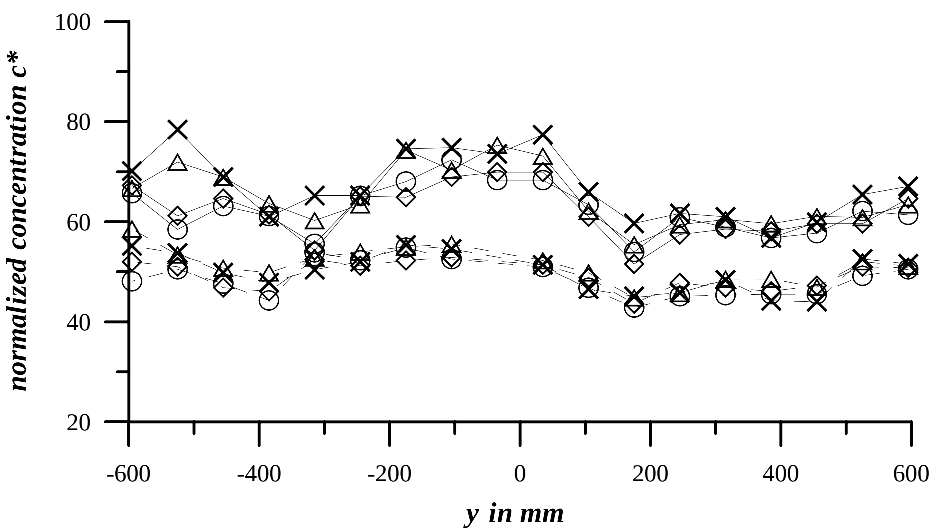

← **Normalized concentration**

$$c^* = \frac{c u_{ref} z_{ref}}{Q_t}, \text{ where } Q_t \text{ is in } [L^2\,T^{-1}],$$

at z = 10 mm and x = 90 mm (solid lines) and x = 180 mm (dashed lines) for four test cases with different wind velocities and source flow rates.

Longitudinal and vertical profiles of normalized concentration

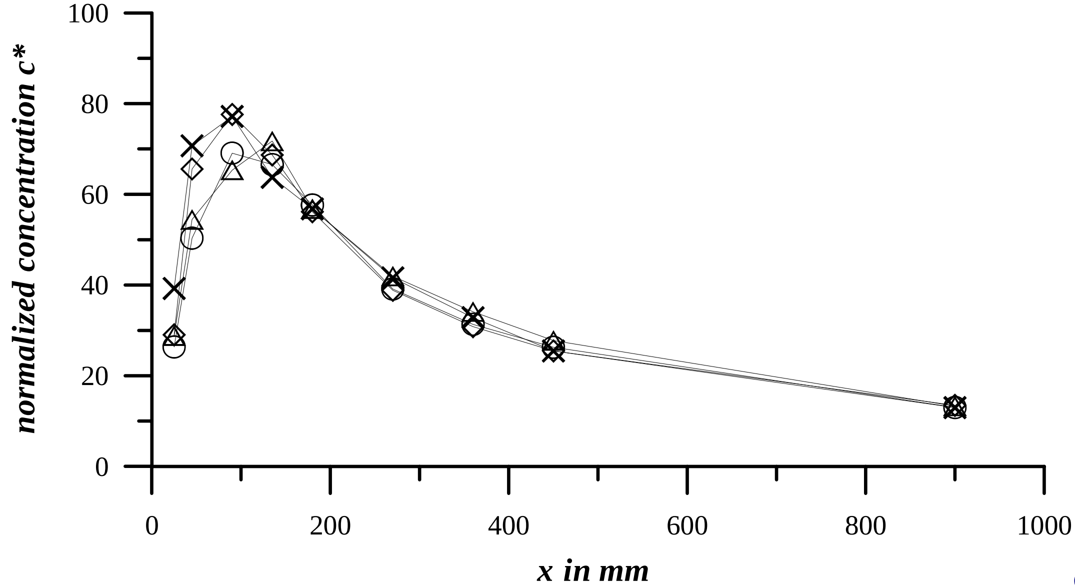

at z=10 mm

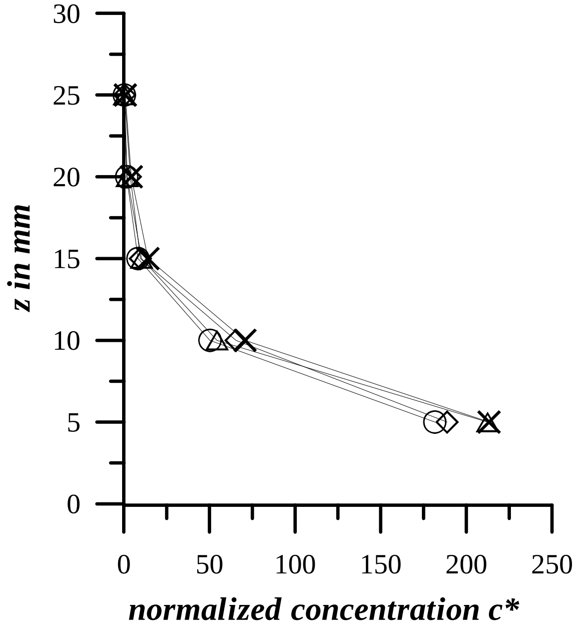

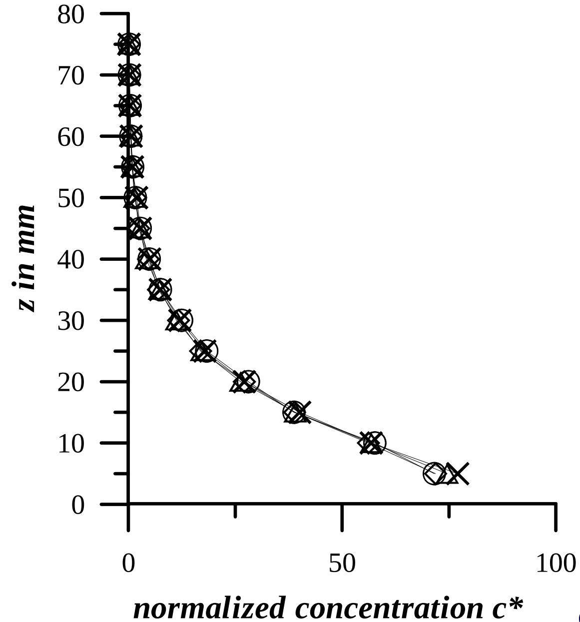

at x=45 mm

at x=180 mm

Numerical model of dispersion from a ground line source

Balance equation for concentration *c* of a passive tracer is solved in a *x*-*z* plane perpendicular to the source located at *x*=0, *z*=0:

$$u(z)\frac{\partial c}{\partial x} = \frac{\partial}{\partial z} K_c(z)\frac{\partial c}{\partial z} + I_s .$$

Mean velocity profile is assumed to be logarithmic: $u(z) = \frac{u_*}{\kappa}\ln\frac{z}{z_0}$.

Eddy diffusivity linearly depends on height as $K_c(z) = \kappa u_* z / \mathrm{Sc}_t$, where Sc_t is the **turbulent Schmidt number**.

Boundary conditions: $\partial c / \partial z = 0$ at $z = z_0$ and *c*=0 at $z = \delta_l$.

Friction velocity is determined from $u_* = \kappa u_l / (\ln \delta_l / z_0)$.

$I_s = Q_s / (\Delta x_1 \Delta z_1)$ is the **source function**, where $\Delta x_1 \Delta z_1$ is the cross-section area of the numerical grid cell surrounding the source. Elsewhere in the model domain outside this cell: $I_s = 0$.

Numerical solution: implicit integration over *x* and factorization over *z*.

Model verification against the wind tunnel data

Ground-level concentration (left plot)

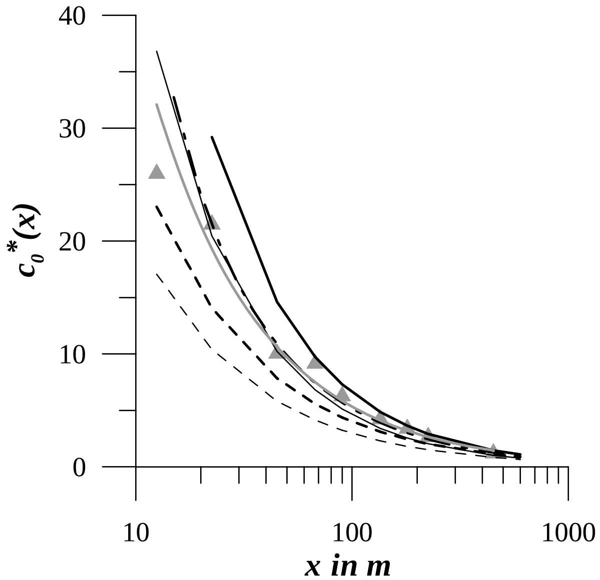

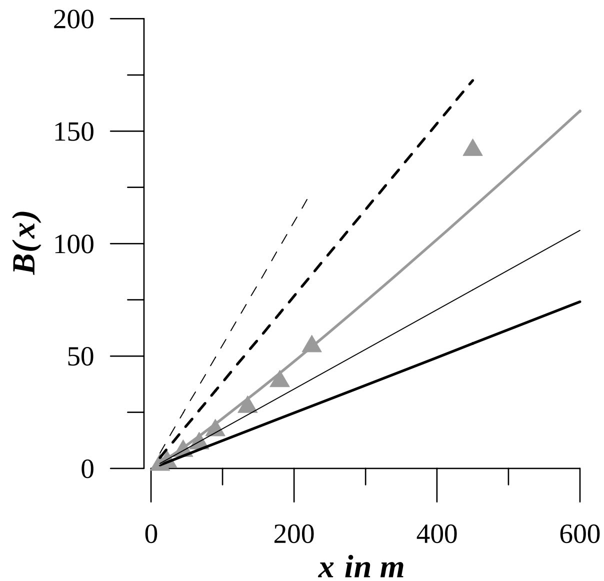

Wind tunnel data are gray symbols and lines.

Dashed-dotted line shows numerical data for $Sc_t = 1$.

Other lines represent different analytical solutions considered in Kastner-Klein and Fedorovich (2002).

Concentration profiles at x = 45 m (left), x = 90 m (center), and x = 180 m (right)

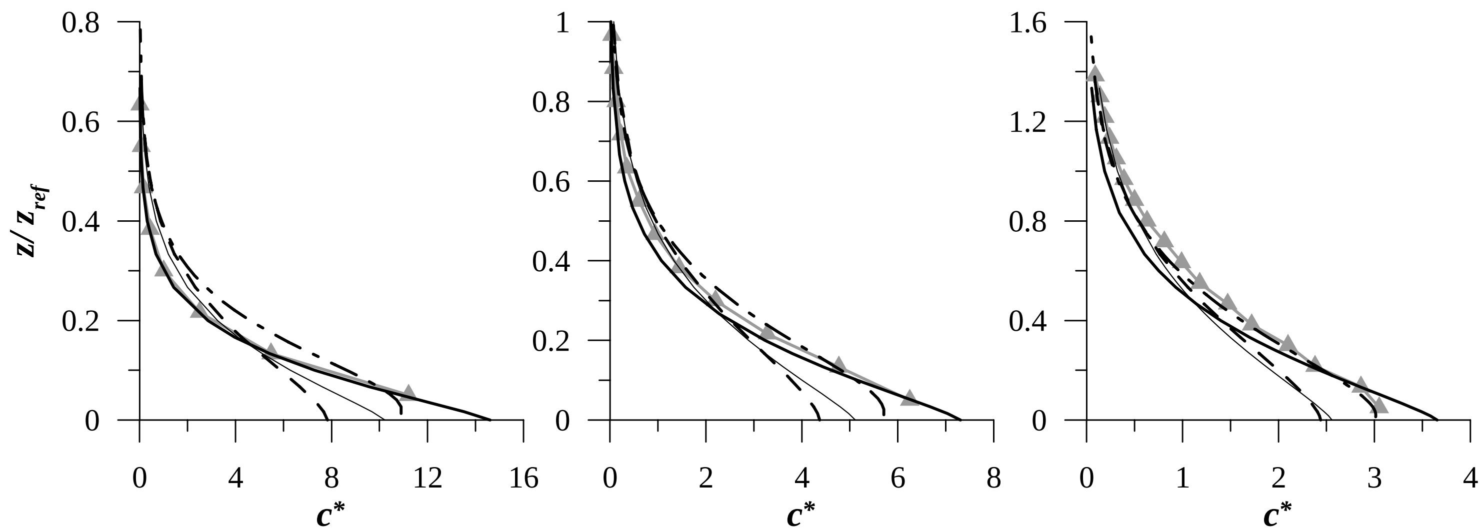

Convective boundary layer (CBL) along a heated surface

Dry (or clear) atmospheric CBL is a turbulently mixed boundary layer with the turbulence dominantly forced by heating from below and wind shear representing the secondary turbulence forcing

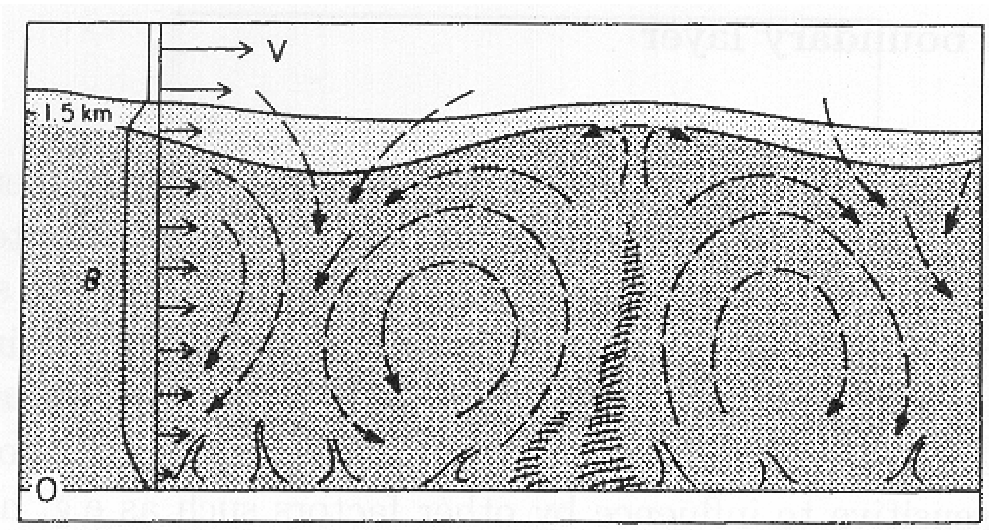

Schematic of temperature and wind fields in the atmospheric CBL (after John Wyngaard)

CBL without wind shear

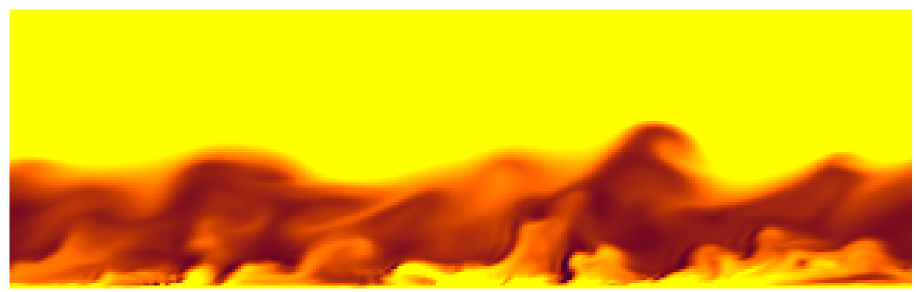

CBL with wind shear

Potential temperature field in the inversion-capped CBL (DNS visualization)

Wind tunnel model of a horizontally evolving atmospheric CBL

Experimental setup in the thermally stratified wind tunnel of UniKA

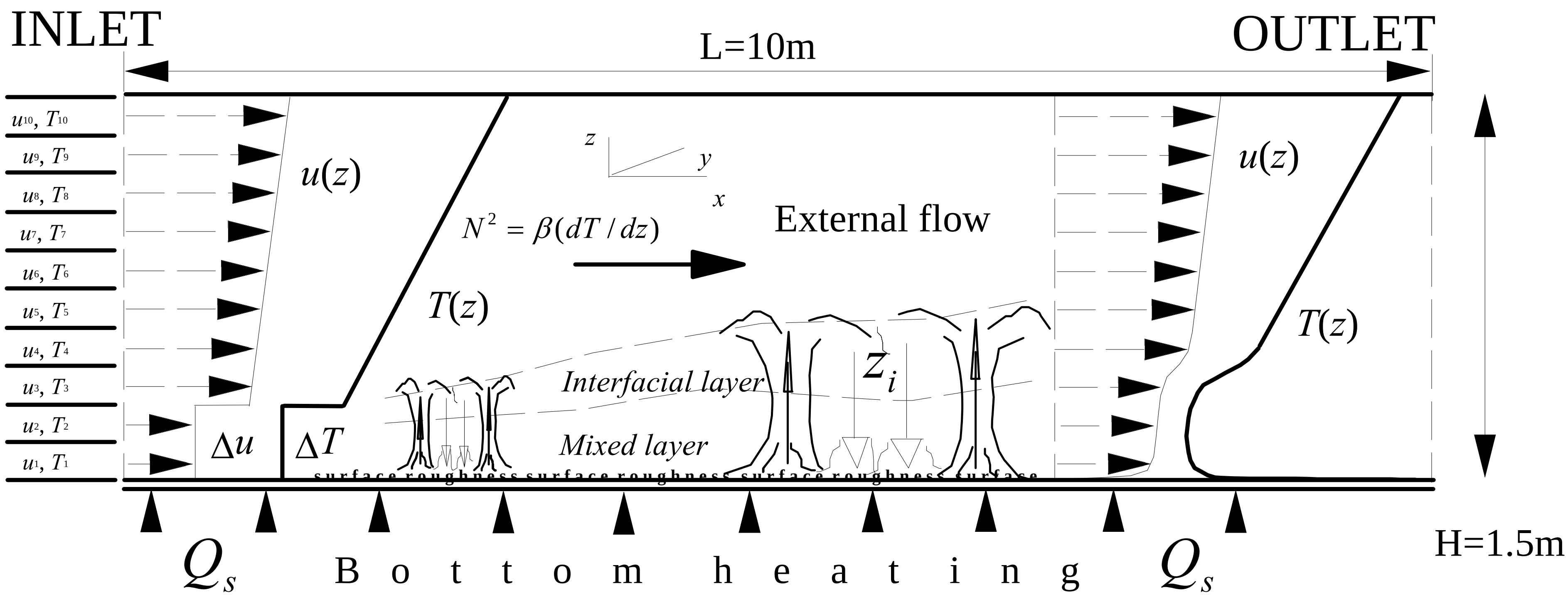

Richardson numbers: $\mathrm{Ri}_{\Delta T} = \beta w_*^{-2} z_i \Delta T$ and $\mathrm{Ri}_N = N^2 z_i^2 w_*^{-2}$

Shear/buoyancy forcing ratio: u_* / w_*, where $w_* = (\beta Q_s z_i)^{1/3}$

Atmospheric CBL: $\mathrm{Ri}_{\Delta T}$<100 Ri_N<100 u_* / w_*<1

UniKA wind tunnel: $\mathrm{Ri}_{\Delta T}$<10 Ri_N<20 $u_* / w_* \approx 0.3$

Water tank, D-W: $\mathrm{Ri}_{\Delta T}$=15 Ri_N=100 u_* / w_*=0 (shear-free CBL)

UniKa thermally stratified wind tunnel

Interior of the tunnel

Exterior of the tunnel

Visualized CBL flow

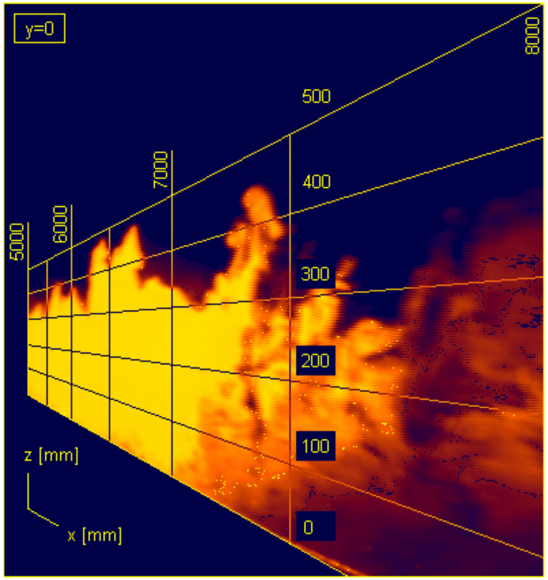

Visualized neutral BL flow

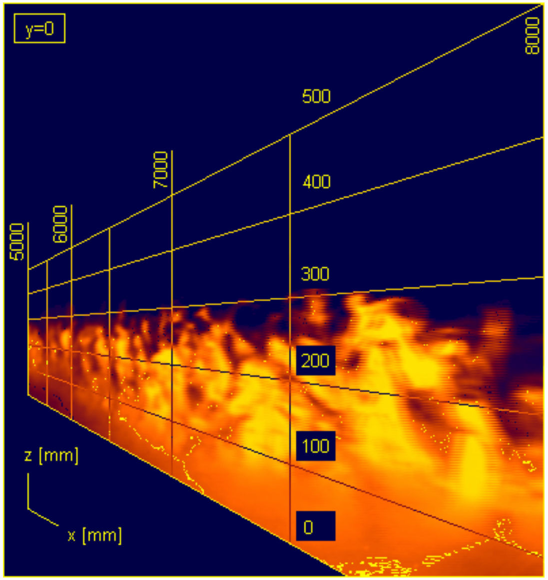

Flow evolution in the UniKa wind tunnel model of CBL

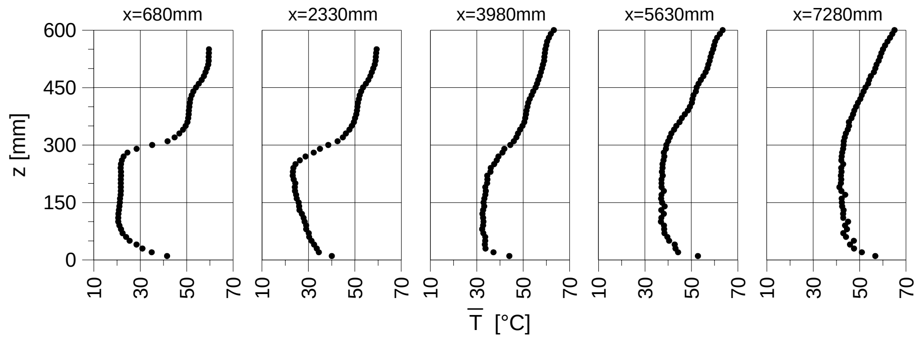

Mean temperature

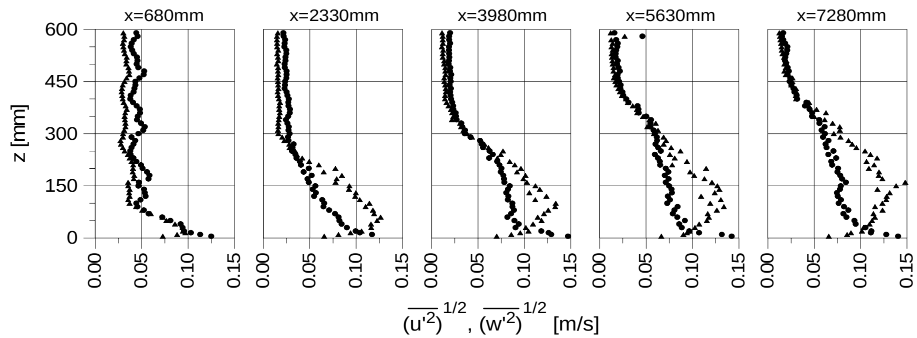

Velocity fluctuations

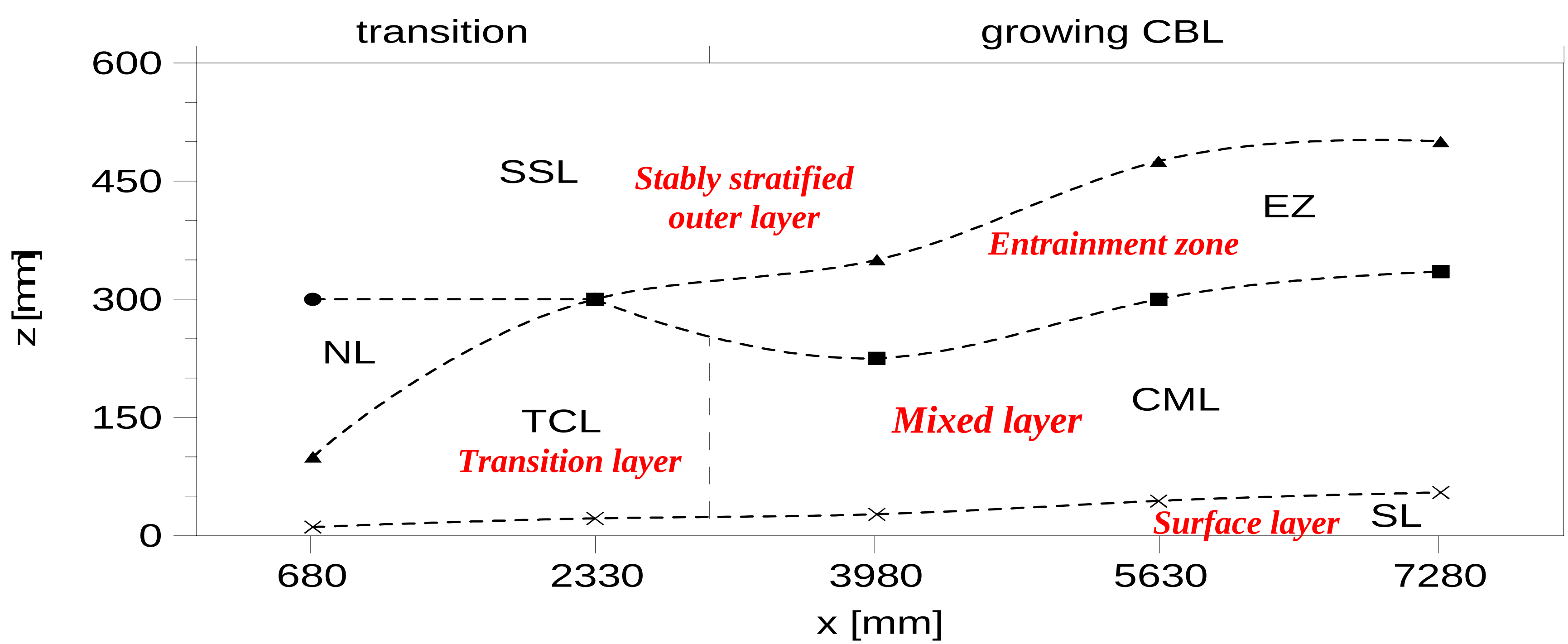

Sublayers within the modeled CBL and flow evolution stages

Large eddy simulation of horizontally evolving CBL

Parameter	Setting
Domain size	10×1.5×1.5m^3 (UniKA WT test section)
Grid	400×60×60
Surface kinematic temperature flux	1 K·m·s^{-1}
Temperature stratification above CBL	33 K·m^{-1}
Time advancement	Leapfrog scheme with a weak filter
Outflow boundary conditions	Radiation conditions for prognostic variables + mass-flux outflow correction
Lateral and top boundary conditions	No-slip + log wall law for velocity; zero-gradient for other prognostic variables
Inflow boundary conditions	Preset stationary fields of mean velocity and temperature with superimposed non-correlated random fluctuations of prescribed r.m.s. magnitude
Bottom boundary conditions	No-slip for velocity; zero-gradient for other prognostic variables; Monin-Obukhov similarity functions implemented locally to relate surface fluxes and gradients
Subgrid turbulence closure	Subgrid TKE-based (Deardorff 1980)

Visual comparison of simulated and modeled (WT) flows

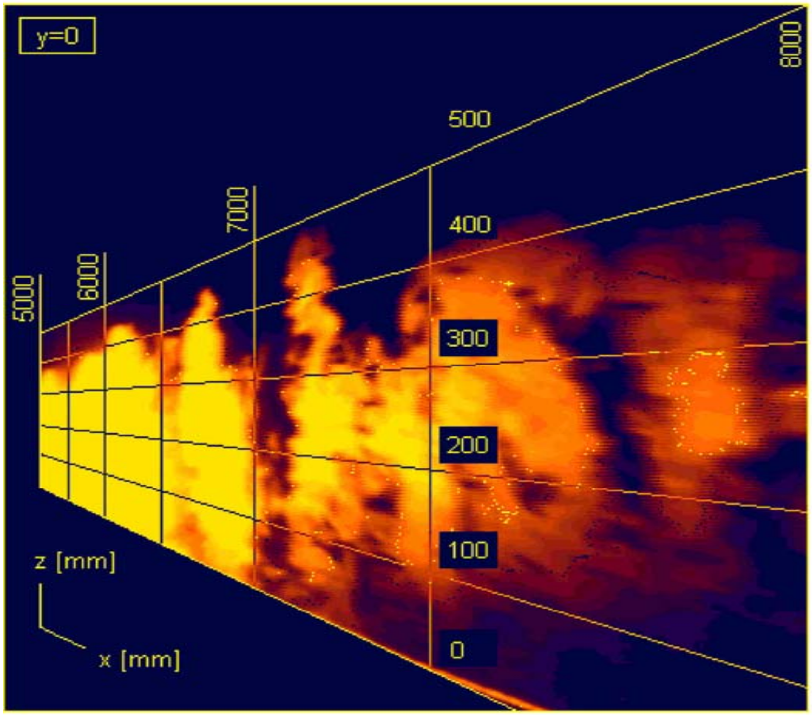

Visualization in the wind tunnel

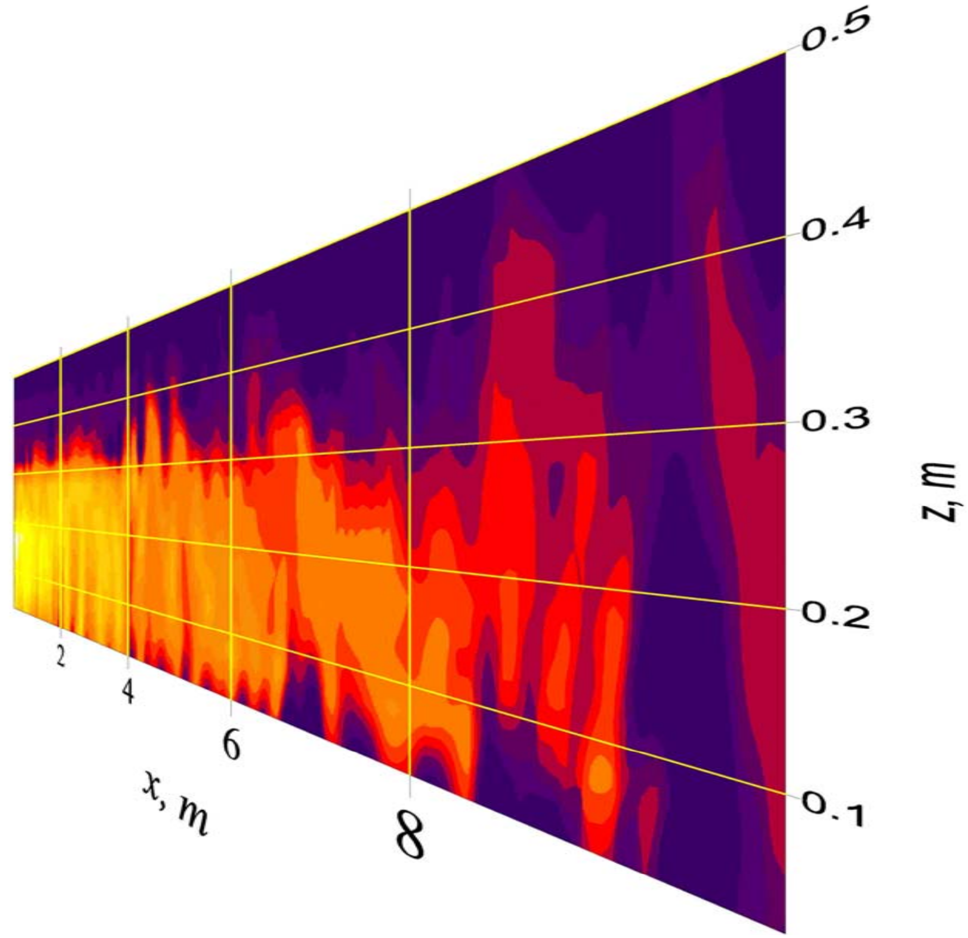

Temperature pattern from LES

Changes of flow structure across the inversion layer

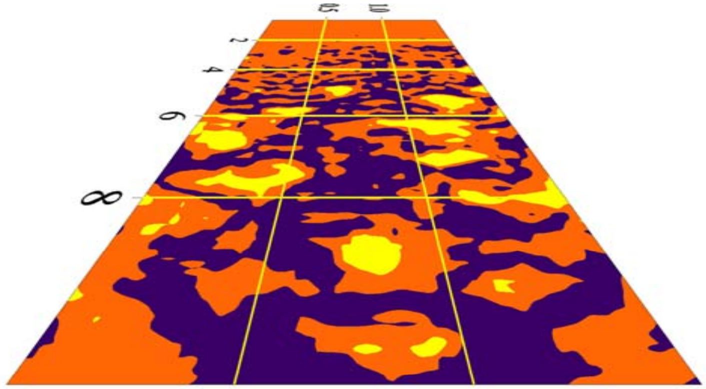

z=0.425m

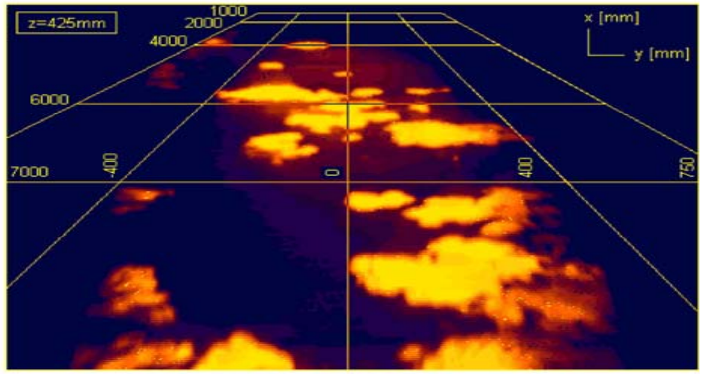

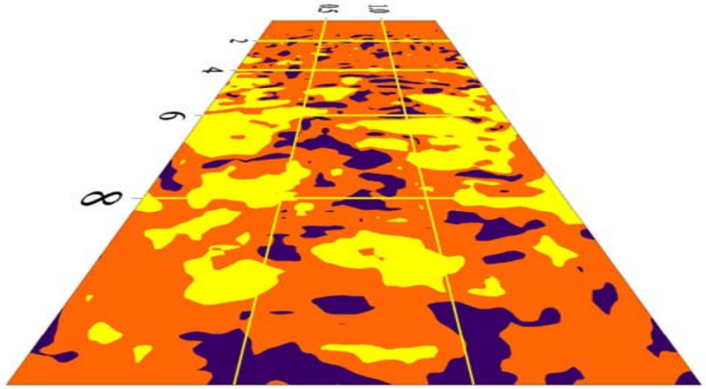

z=0.375m

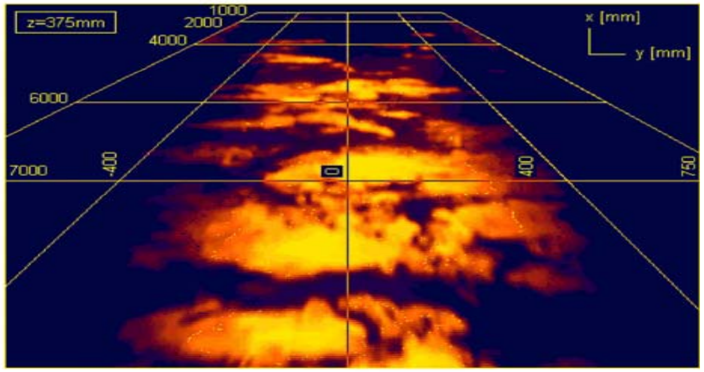

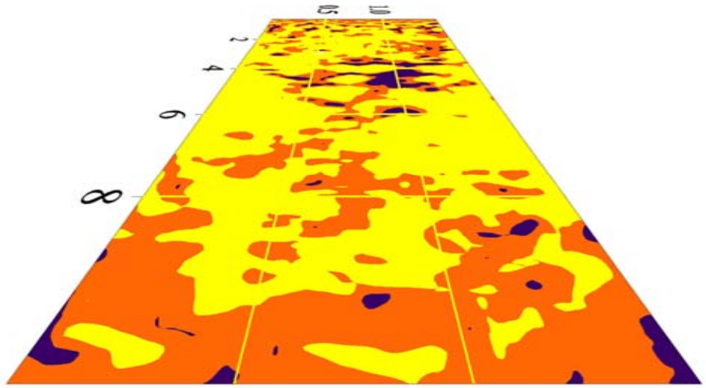

z=0.325m

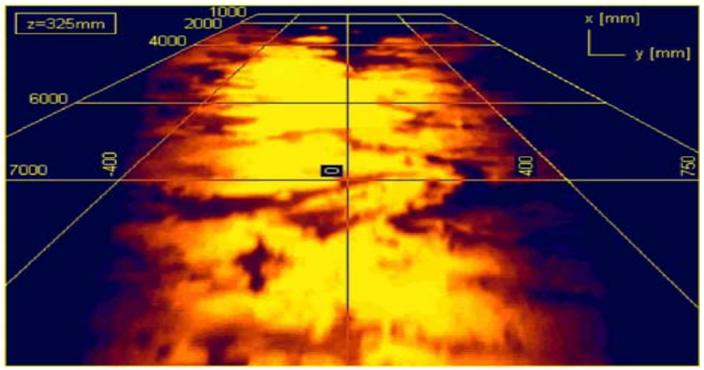

Temperature pattern from LES

Visualization in the wind tunnel

Evolution of flow fields in the wind tunnel CBL: LES data

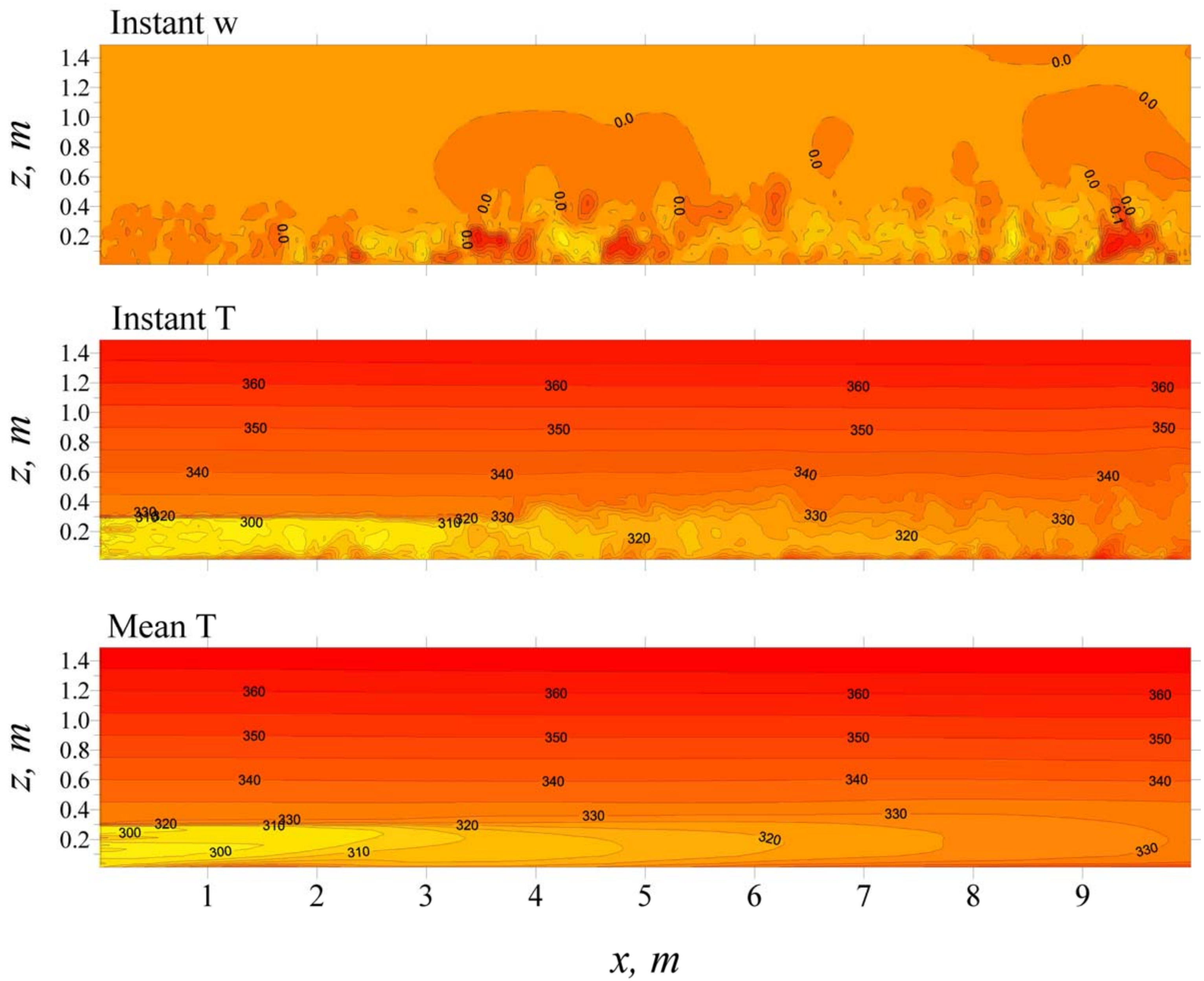

Role of inflow conditions in transition to well-mixed CBL

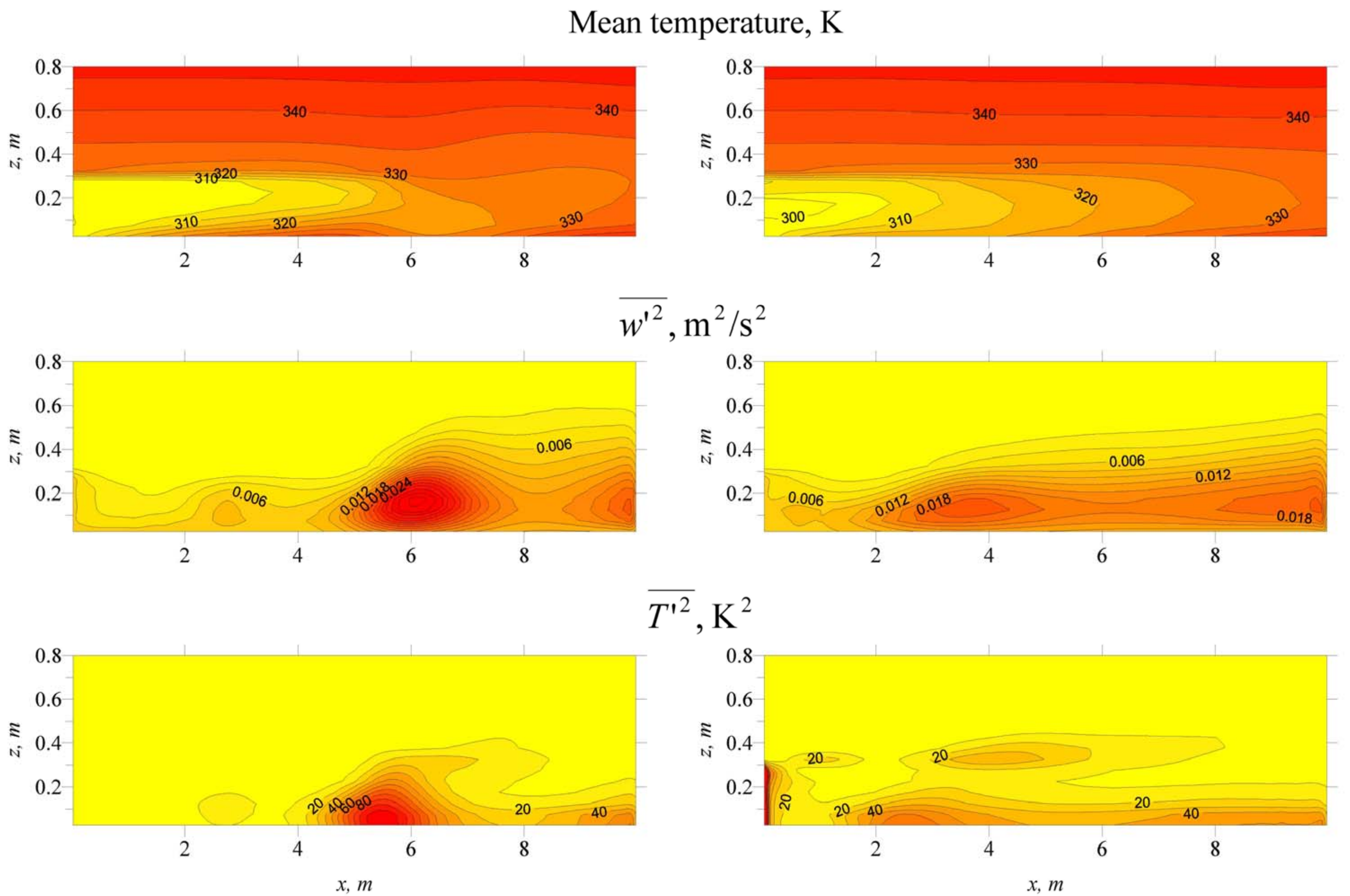

Inflow without disturbances

Inflow temperature agitated below the inversion

Laddering temperature field above CBL by agitating incoming flow

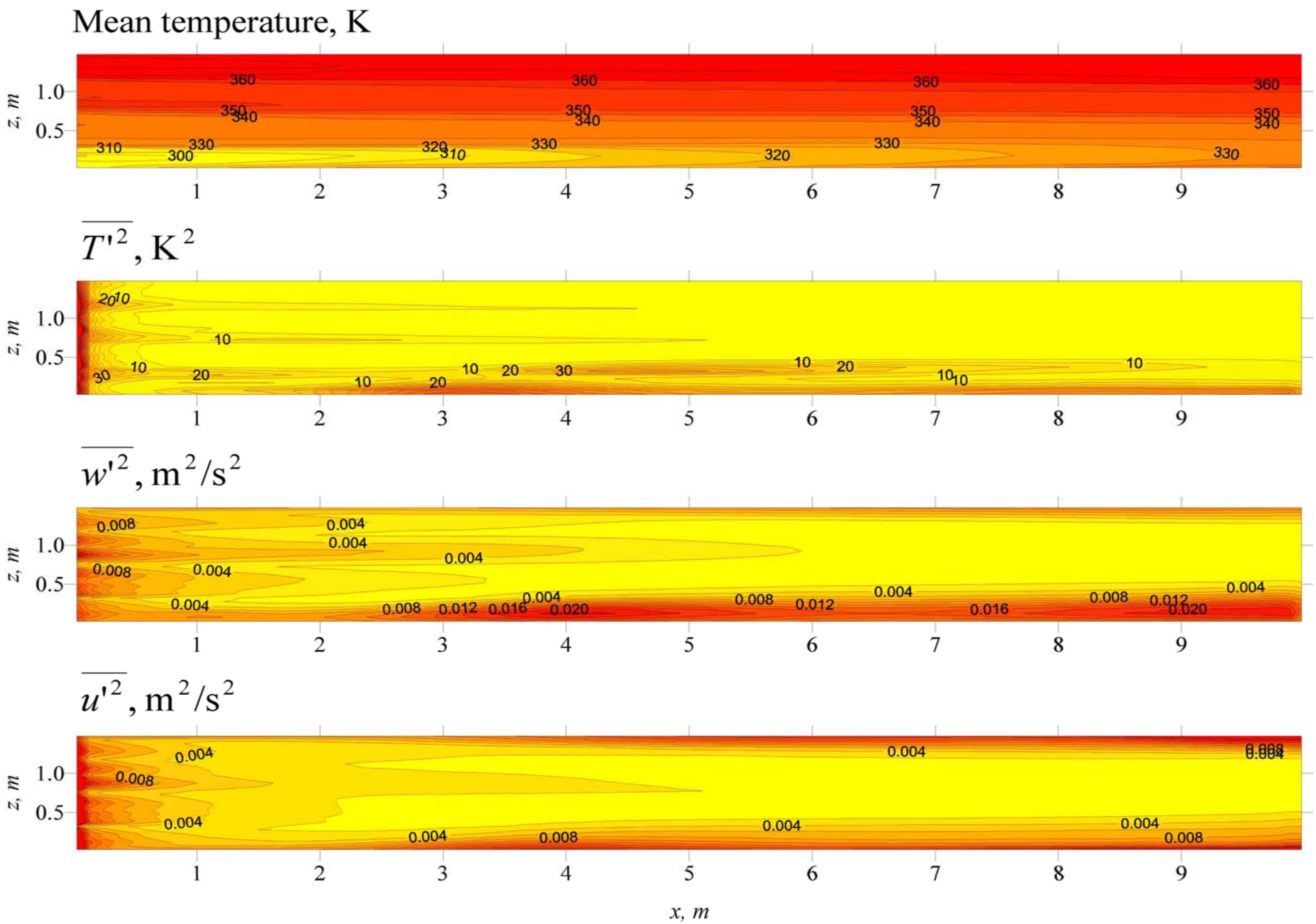

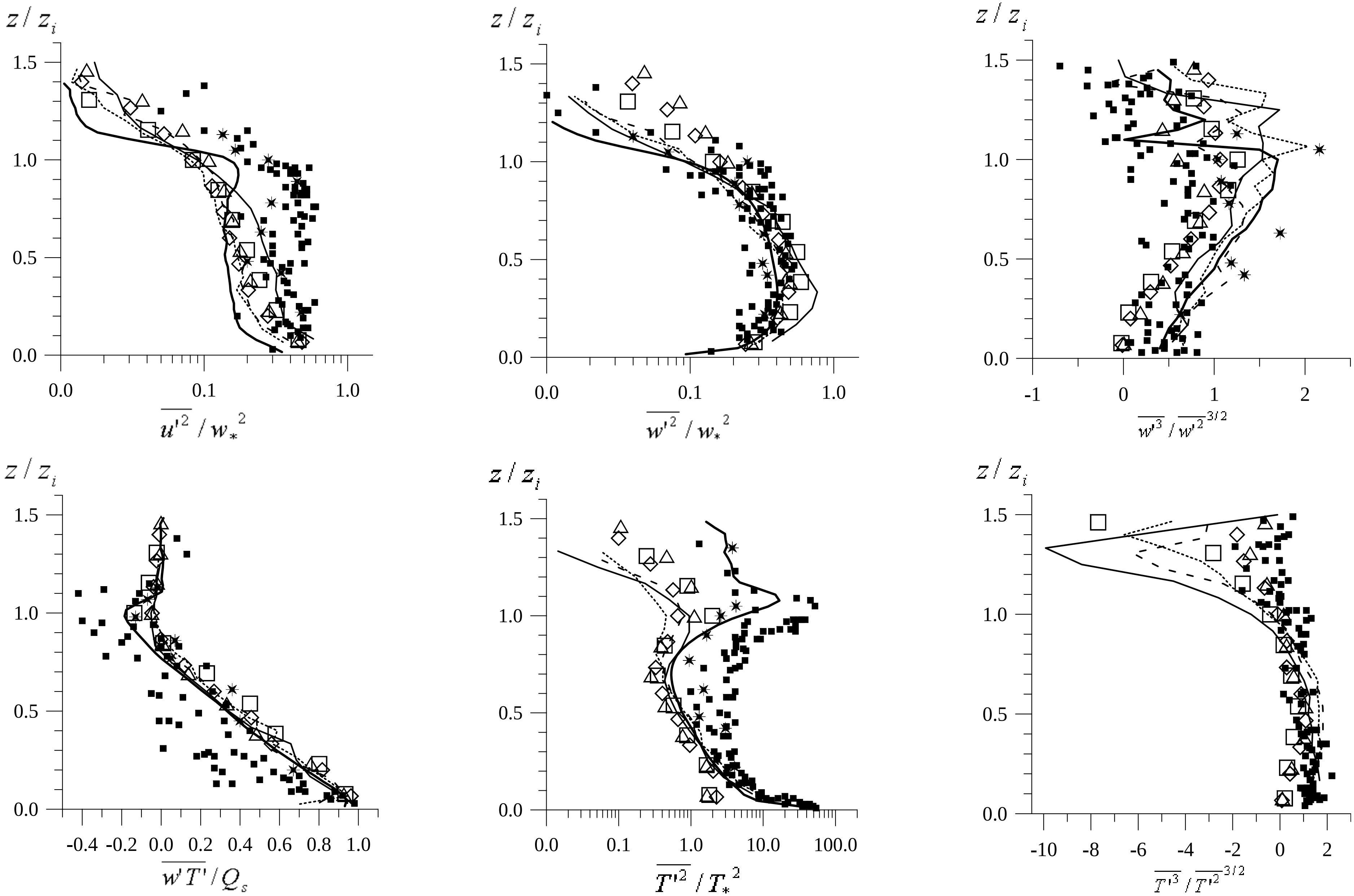

Thin lines: WT (3 windows); **B**old lines: LES (shear-free CBL); **O**pen symbols: LES of WT CBL (3 windows); **F**illed squares: atmosphere; **A**sterisks: water tank.

Effect of elevated shear on the CBL deepening (WT data)

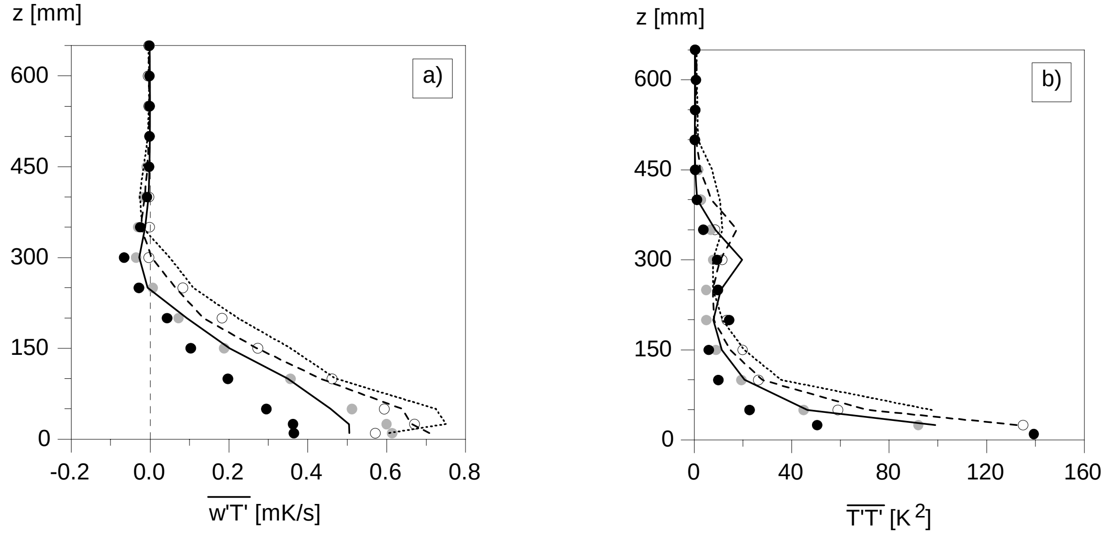

Without elevated shear: lines. In the presence of positive elevated shear: points.

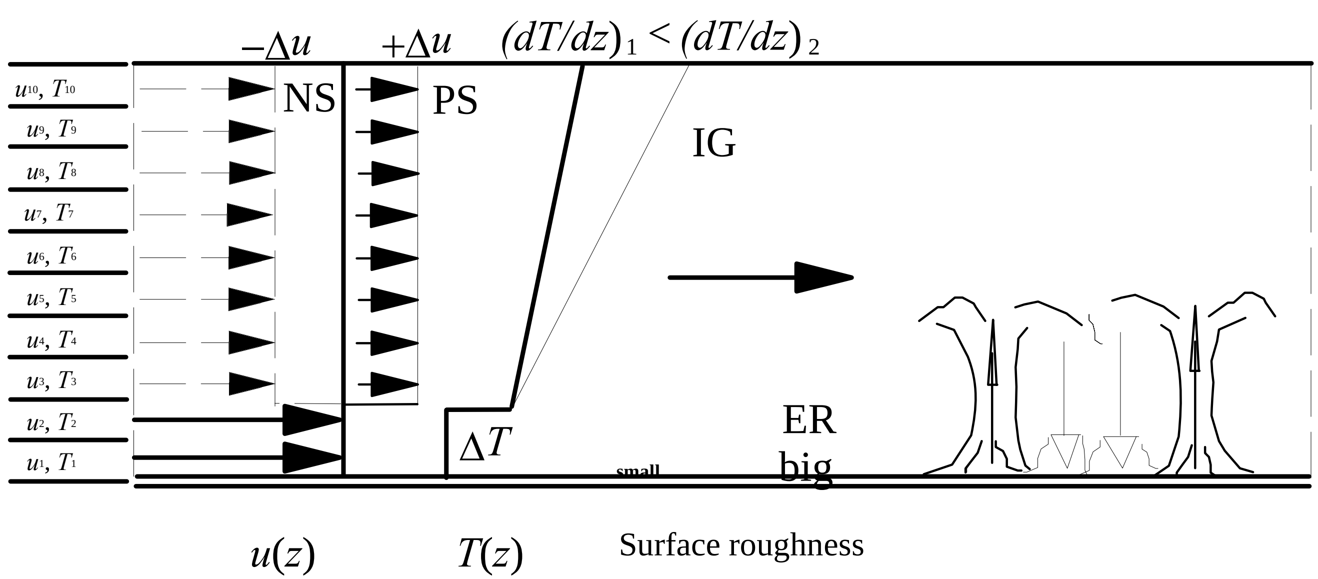

Using LES to study complimentary CBL flow regimes

Elevated shear vs. entrainment in control of CBL growth

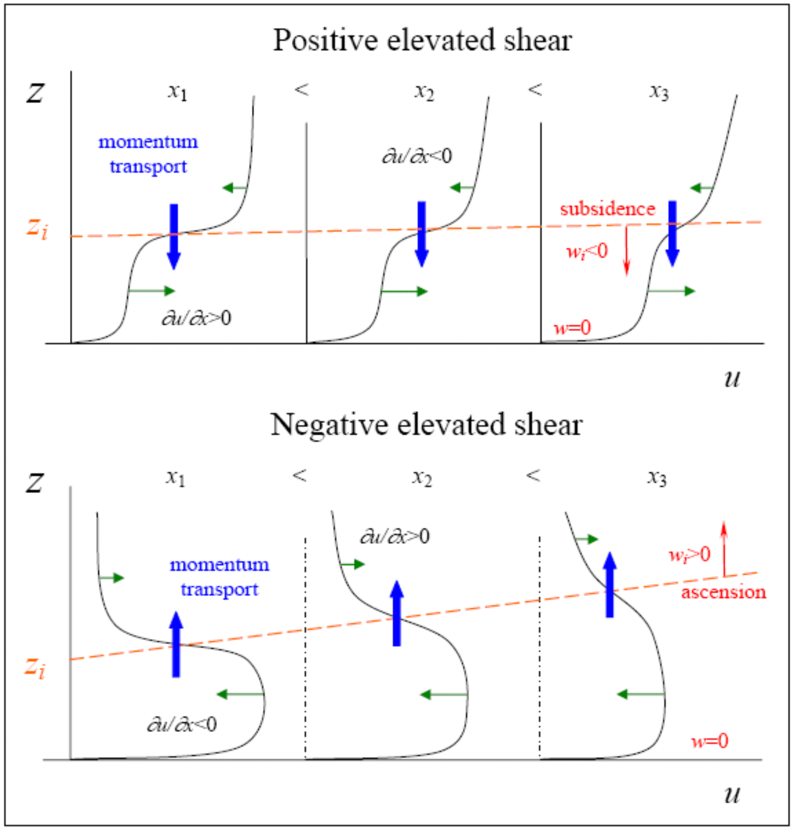

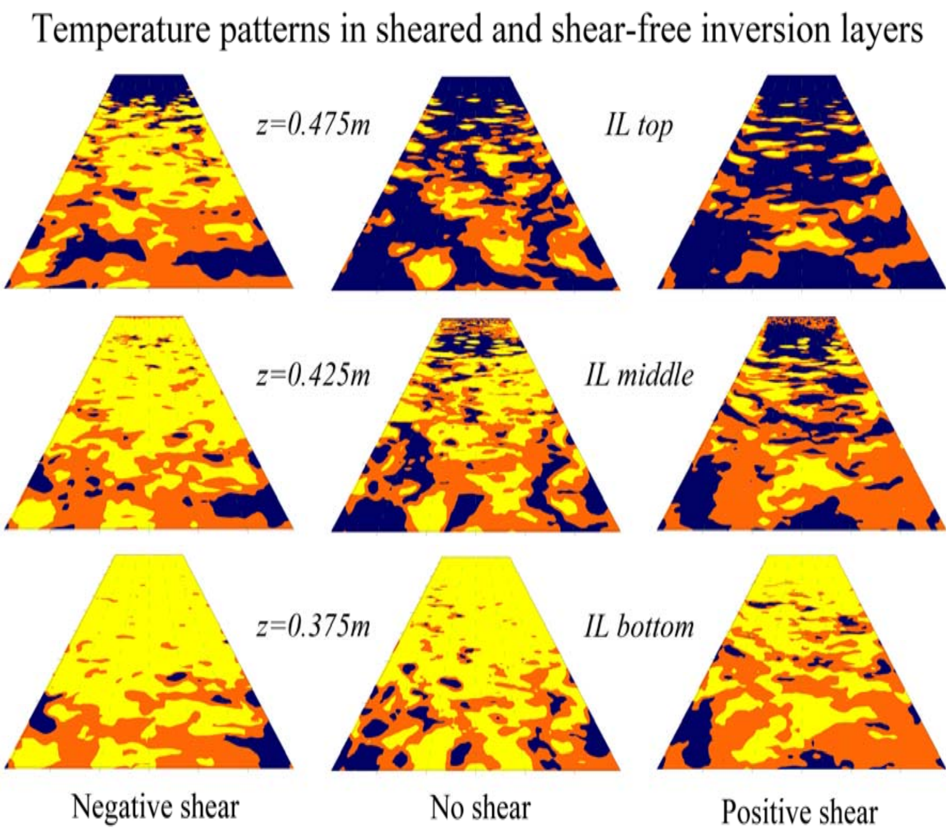

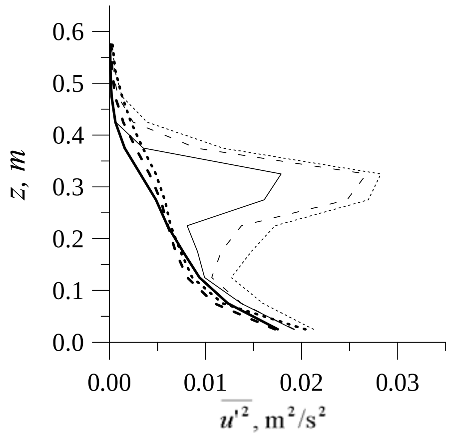

Positive shear

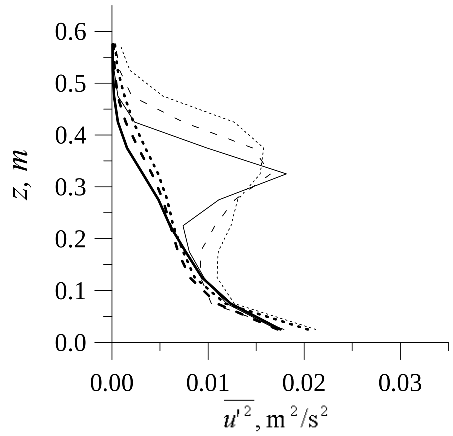

Negative shear

Combining WT modeling and LES to study dispersion in the CBL

Wind tunnel   LES

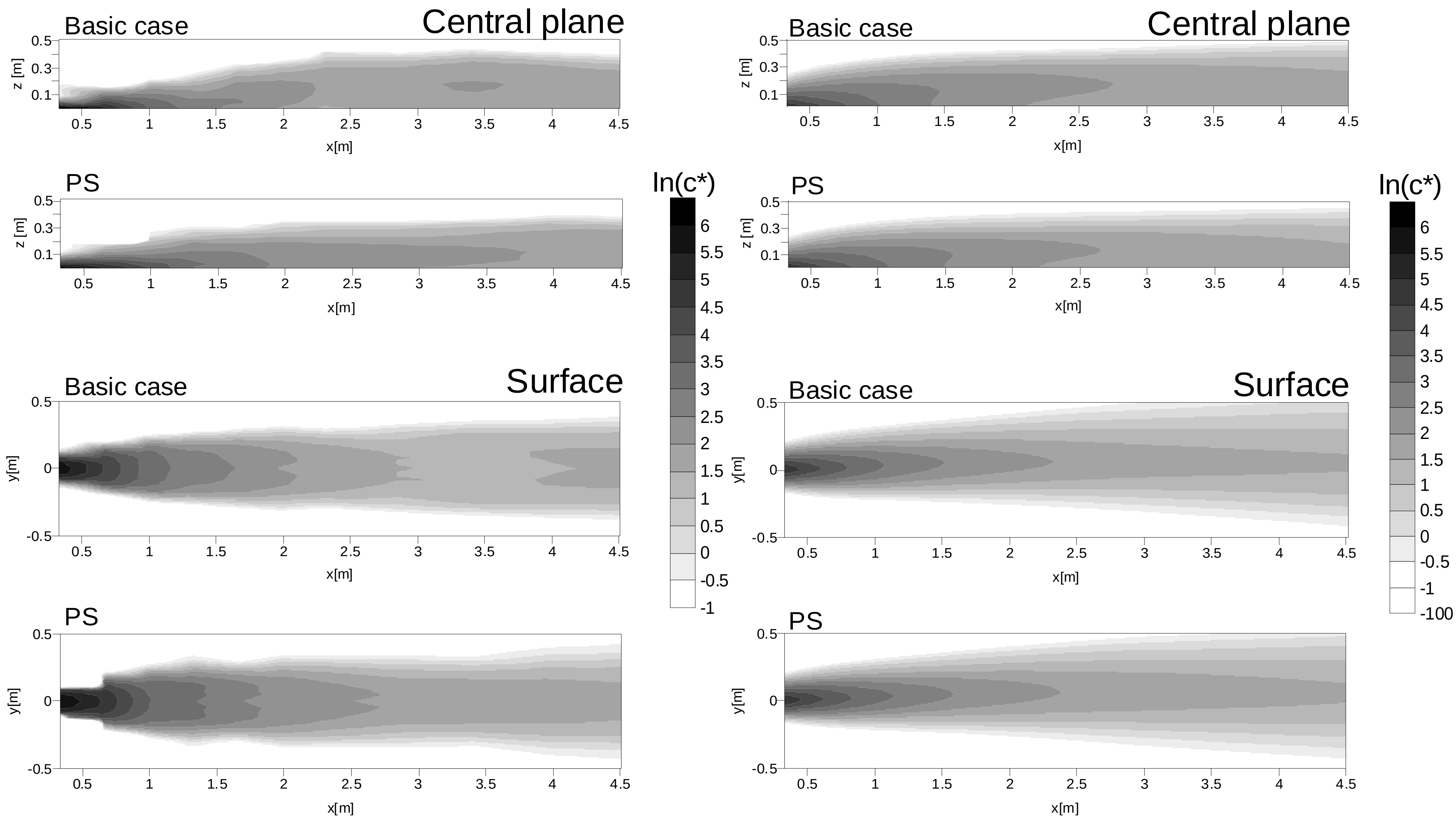

Point source is at the ground level. The origin of the *x* ordinate is at the source location. The capping-inversion and shear-zone elevations at *x*=0 are 0.3 m.

Using WT and LES output to feed Lagrangian dispersion model

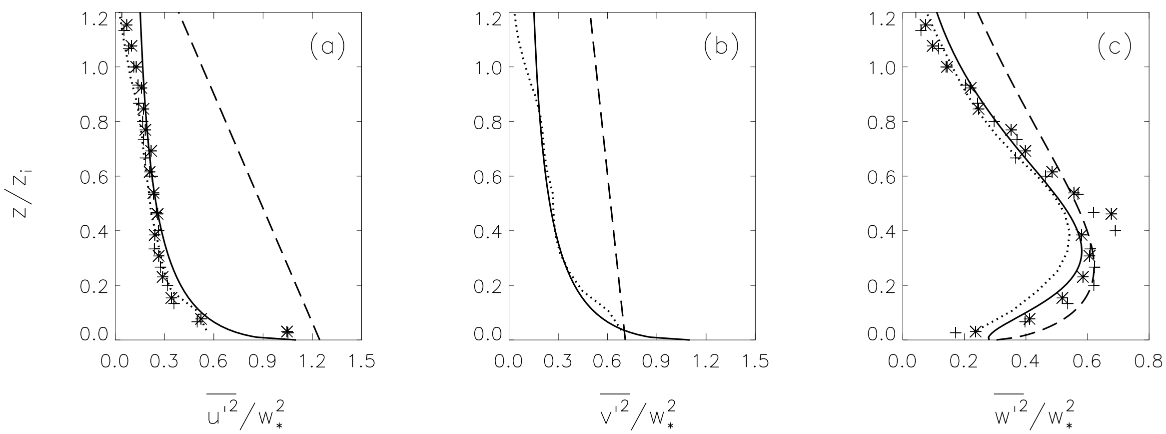

Original (dashed lines) and new (solid lines) **turbulence parameterizations** in the Rotach et al. (1996) Lagrangian dispersion model.

Markers are WT data, dotted lines are LES data.

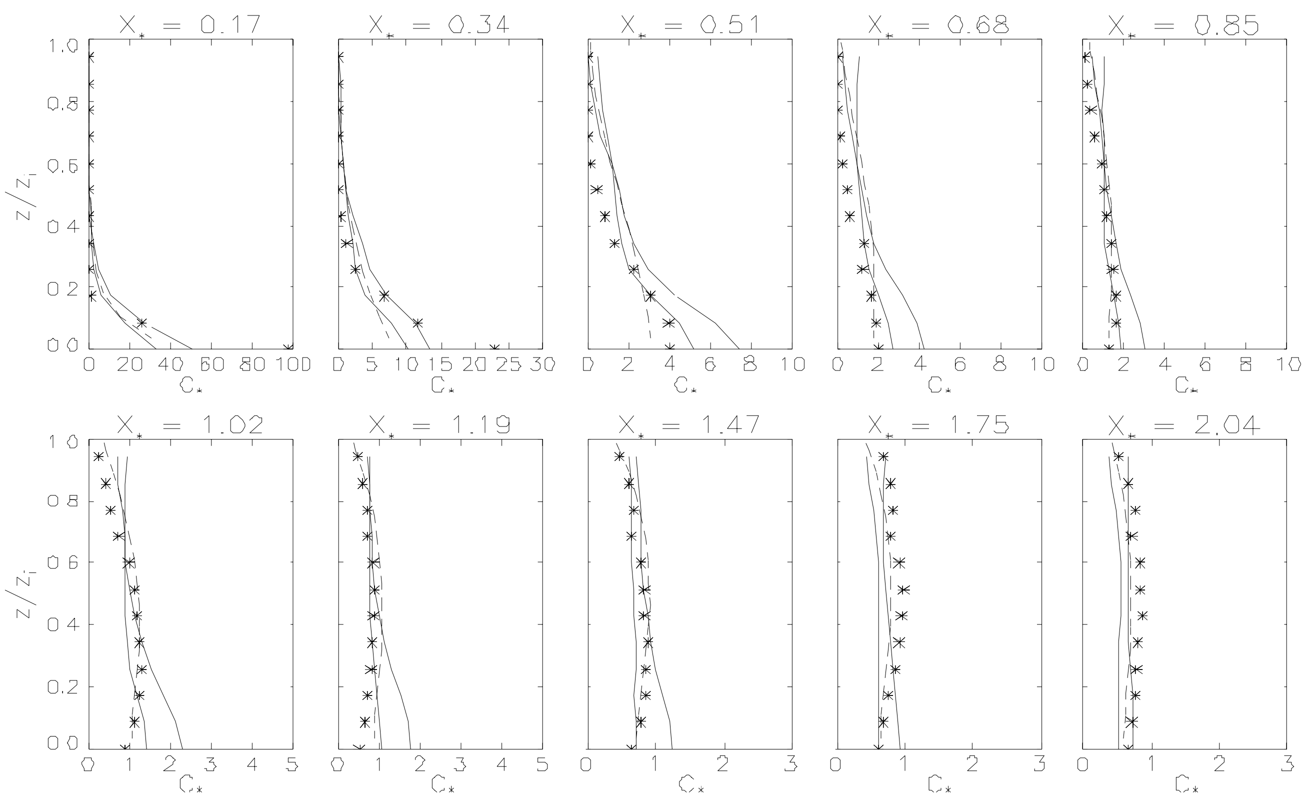

Lagrangian model predictions of plume centerline concentration at different *x* downwind of the ground source.

Solid lines – with new, dashed lines – with old parameterizations

Markers are WT data and short-dashed lines are LES data.

Effect of source elevation on dispersion pattern in CBL (LES visualization)

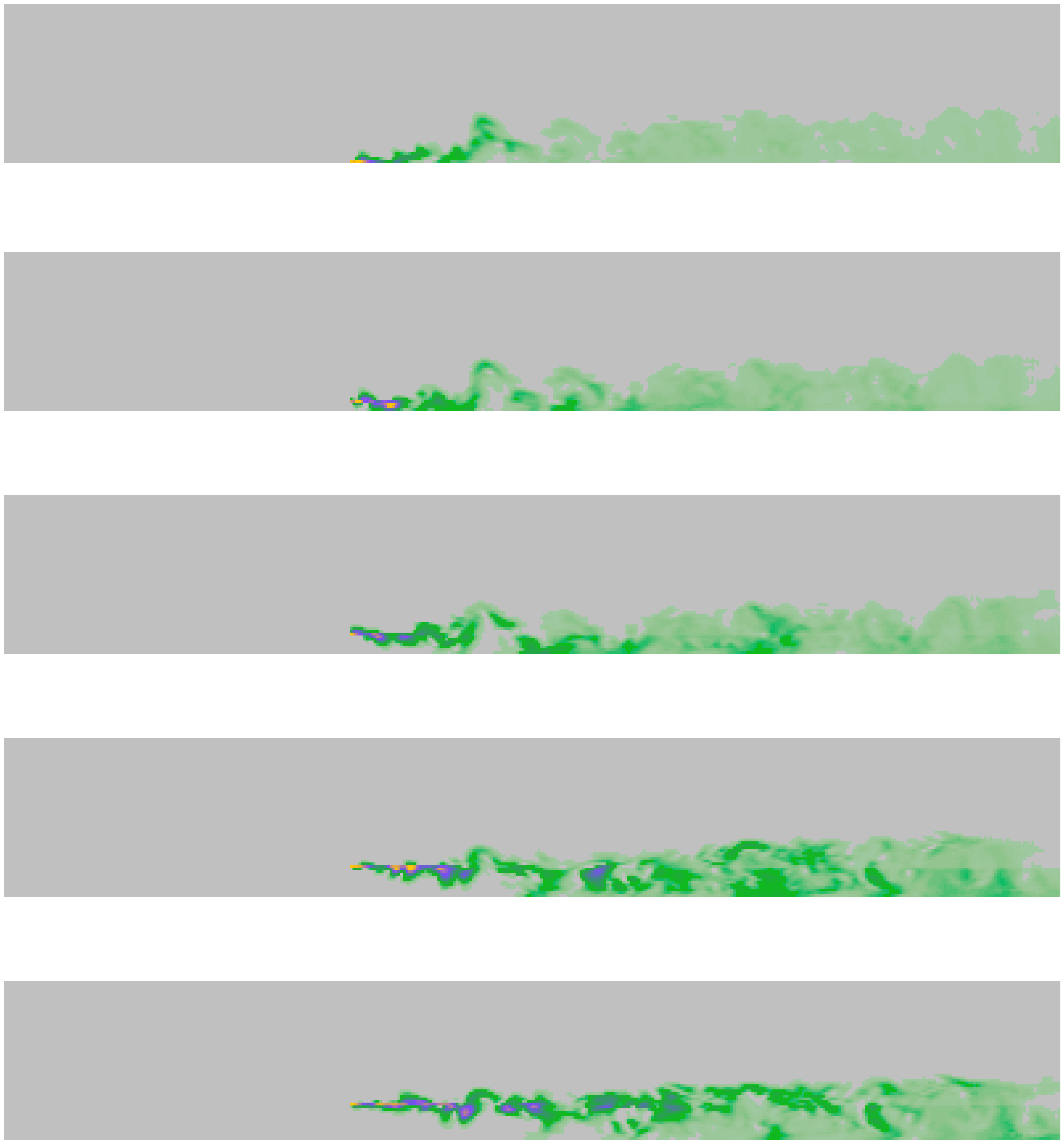

$z_s / z_i = 0$ (ground)

$z_s / z_i = 0.33$

$z_s / z_i = 0.67$

$z_s / z_i = 1$

$z_s / z_i = 1.17$

Laboratory studies deserve higher priority in our research agenda. Simply making this point is a big challenge, however, in a time when we are so overwhelmingly occupied with numerical modeling and simulation

John Wyngaard

References

Kastner-Klein, P., and E. Fedorovich, 2002: Diffusion from a line source deployed in a homogeneous roughness layer: interpretation of wind tunnel measurements by means of simple mathematical models. *Atmospheric Environment*, **36**, 3709-3718.

Fedorovich, E., F. T. M. Nieuwstadt, and R. Kaiser, 2001: Numerical and laboratory study of horizontally evolving convective boundary layer. Part I: Transition regimes and development of the mixed layer. *J. Atmos. Sci.*, **58**, 70-86. Part II: Effects of elevated wind shear and surface roughness. *J. Atmos. Sci.*, **58**, 546-560.

Fedorovich, E., and J. Thäter, 2002: A wind tunnel study of gaseous tracer dispersion in the convective boundary layer capped by a temperature inversion. *Atmospheric Environment*, **36,** 2245-2255.

Fedorovich, E., 2004: Dispersion of passive tracer in the atmospheric convective boundary layer with wind shears: a review of laboratory and numerical model studies. *Meteorol. Atmos. Phys.*, **87**, 3-21.

Thanks go to Rolf Kaiser, Petra Klein, Bernd Leitl, Frans Nieuwstadt, Johannes Thäter, Erich Plate, Matthias Rau, and Mathieu Pourque